Physical and Spectral Analysis of a Semi-Infinite Grounded Slab Illuminated by Plane Waves

Vito Daniele, Guido Lombardi, *Senior Member, IEEE*, and Rodolfo S. Zich, *Honorary Member, IEEE*

***Abstract*— In this article, we study the scattering problem of a truncated grounded slab illuminated by an arbitrarily incident E_z-polarized plane wave. We present a solution using the novel semianalytical spectral method based on an original extension of the Wiener–Hopf (WH) technique that uses the concept of characteristic Green's function and the Fredholm factorization technique. The combination of these mathematical tools allows to extend the capabilities of classical WH method to a new set of problems. One of the main benefits of the proposed semianalytical solution is that it allows the computation of field components similar to what is done with closed-form spectral solutions when available. Physical phenomena, such as the reflection, diffraction, and excitation of surface/leaky waves, are reported. Numerical results validate the proposed methodology.**

***Index Terms*— Antenna technologies, dielectric waveguide, electromagnetic diffraction, electromagnetic scattering, Green's function, grounded slab, integral equations, leaky waves, near-field interactions, optics, radar, surface waves, Wiener–Hopf (WH) method.**

I. Introduction

THE accurate analysis of electromagnetic scattering by a truncated grounded slab constitutes a fundamental canonical problem with applications in radar technology, planar antenna design, optics, and surface propagation in substrate technology.

In computational electromagnetics, both in full numerical techniques and semianalytical ones available up today, a thorny topic is the correct modeling of near-field interaction among thin structures, edges, penetrable interfaces, and conducting bodies. However, often, a closed-form analytical solution of practical problems is not available in the literature, as for the structure proposed in this article. The literature reports a variety of approximate methods to study the problem with different drawbacks.

Full numerical techniques, such finite methods and method of moments, can be difficultly applied due to the infinity of the structure and due to the closeness of diffraction structures, where physical phenomena need to be correctly modeled for the presence of different materials with critical sharpness and thickness. Moreover, the application of approximate boundary condition formulations [1], [2], [3], [4], [5] suffers from limitations of accuracy when the thickness of the penetrable material becomes large in terms of wavelength or when the density of the penetrable material becomes low. The literature also reports solution by means of physical optics (PO) [6], [7]. Variational techniques based on modal analysis and mode matching analysis in similar problems are reported in [8]. For an accurate study of the structure, rigorous integral equation formulations have been applied in [9], [10], [11], [12], and [13], but they require a considerable computational effort.

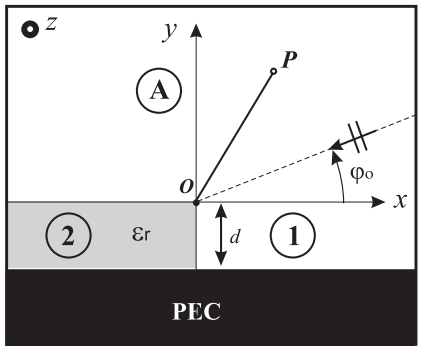

Fig. 1. Electromagnetic plane wave scattering of a truncated penetrable layer grounded by a PEC plane immersed in a second different homogeneous medium. We define three regions: 1) $x > 0$, $-d < y < 0$, 2) $x < 0$, $-d < y < 0$, and A) $y > 0$.

In the framework of the Wiener–Hopf (WH) technique, we report works dealing with structures similar to one of this article [14], [16] and with the structure object of this article [1], [15], [17]. However, most of these works consider sources near the slab or the scattering of surface waves.

In this article, we present a novel semianalytical solution of the problem using an extended version of the WH technique. We obtain a solution for the scattering of plane waves that can be extended to more complex sources with plane wave expansion as reported also in [19] where the problem is analyzed by means of analytical–numerical techniques based on integral equation formulation and the method of moments.

The proposed novel semianalytical method is based on the WH technique combined with the Fredholm factorization method [20], [21] that allows the study of the problem independently of the thickness and the density of the penetrable semi-infinite layer correctly considering near-field interaction. In particular, we note that the WH literature on similar problems reports procedures based on Jones's like methods (see [21], [22], [23], [24], [25], [26], [27], [28]) where a system of infinite equations is solved approximately to get the solution of the modified WH problem. This method was adopted in particular in [15], [16], [17], and [18] where an ad hoc prefactorization of scalar functions is needed.

Manuscript received 4 April 2022; revised 3 August 2022; accepted 14 September 2022. Date of publication 5 October 2022; date of current version 22 December 2022. This work was supported by the Italian Ministry of University and Research (MUR) through "Chipless radio frequency identification (RFID) for GREEN TAGging and Sensing—GREEN TAGS" under the PRIN2017 Grant 2017NT5W7Z. *(Corresponding author: Guido Lombardi.)*

The authors are with the Dipartimento di Elettronica e Telecomunicazioni (DET), Politecnico di Torino, 10129 Turin, Italy, and also with the Istituto Superiore Mario Boella (ISMB), 10129 Turin, Italy (e-mail: vito.daniele@polito.it; guido.lombardi@polito.it; rodolfo.zich@torinowireless.it).

Digital Object Identifier 10.1109/TAP.2022.3210704

In this article, we present an alternative and more versatile method based on incomplete WH equations formulated by using the characteristic Green's function procedure. Some preliminary and incomplete formulation is reported in [29] and [30]. Furthermore, a detailed analysis of the properties of Green's formulation combined with the Fredholm factorization method [20], [21] yields explicit Fredholm integral equations (FIEs), (69) and (70), in terms of the spectral WH unknowns. We note also that to get these FIEs, a prefactorization of scalar functions is not necessary. We observe that the explicitness of the formulation is a great advantage with respect to the approximate solution based on the infinite linear system of equations that require a multistep analysis for the convergence as applied in [31] for a different but mathematically similar problem. In particular, we note that the application of Cauchy integral representation allows to avoid the formulation in terms of infinite system of equations. Furthermore, we observe that the application of Fredholm factorization allows to get regularized integral representations with compact kernels.

The new proposed methodology has the advantage of being independent of the thickness and the density of the materials. Moreover, the proposed method describes the complete structure with a comprehensive mathematical model in the spectral domain avoiding multiple steps of interaction among separated structures. As a result, we obtain the true spectra of field components from which we extract by asymptotics physical/engineering phenomena excited by the structure like in closed-form analytical solutions. In fact, the plane wave illumination excites all the spectra of the grounded truncated penetrable slab for the presence of sharp material-geometrical discontinuities, and by our method, we can analyze the individual physical phenomena.

Applications to radar, antenna technologies, and optics based on layered structures can benefit from this method in particular for the analysis of phenomena such as scattering, surface/leaky waves excitation in substrate technology. Our results can be of utility to exploit the leaky/surface wave capabilities of the structure for planar antenna applications [32], [33], [34], [35], [36], [37], [38], [39]. Beyond the fundamental computation of far field, we estimate also near-field phenomena as surface waves, which can be of interest for coupling phenomena.

This article is organized into nine sections and one appendix. In Section II, we introduce the geometry of the problem and the mathematical background in the spectral domain (Laplace transforms). In the development of the method, we consider the semi-infinite layer made by a dielectric material, and however, the method can be extended to magnetic material, metamaterials [40], [41] on metasurfaces [42], and different physics (acoustic, elasticity, and so on), but these interesting applications are beyond the scope of this fundamental article. Section III presents the mathematical formulation of the problem in terms of incomplete WH equations using a particular application of the characteristic Green's function procedure [43], while Section IV describes the procedure to render complete the equations. The solution procedure based on the application of the Cauchy integral representation and the Fredholm factorization method is reported in Sections V and VI, respectively. Section VII illustrates how to compute physical/engineering quantities by asymptotics as geometrical theory of diffraction (GTD) and uniform theory of diffraction (UTD) field components, total far fields, surface waves, and leaky waves at near and far distance. In Section VIII, we provide validation and convergence of the proposed method. We first compare our solution in the special case of perfectly electrically conducting (PEC) material with the solution obtained by Jones's method [23], [59]. We then compare our results for particular setups with the ones obtained with a fully numerical technique embedding singular modeling [44]. With this comparison, we demonstrate the superiority of the proposed semianalytical technique for canonical problems with approximately infinite canonical geometry and extreme parameters, while numerical techniques well deserve for a finite geometrical model. Finally, conclusions are reported in Section IX.

II. Description of the Problem and Mathematical Statements

In this article, we examine the electromagnetic plane wave scattering of a truncated penetrable homogeneous layer grounded by a PEC plane immersed in a second different homogeneous medium. For simplicity, we assume that the layer is made by a dielectric material and the space around by vacuum, and however, the method is not restricted to this kind of media. We recall that the method can be extended to magnetic material, metamaterials, and different physics (acoustic, elasticity, and so on) as stated in Section I.

The structure is presented in Fig. 1. The free-space region is characterized by the impedance $Z_o = \sqrt{\mu_o/\varepsilon_o}$ and the propagation constant $k = \omega\sqrt{\mu_o\varepsilon_o}$, where ε_0 and μ_0 are, respectively, the absolute dielectric permittivity and the absolute magnetic permeability of free space. The dielectric medium (subregion 2) is defined by the characteristic impedance $Z_d = Z_o/\sqrt{\varepsilon_r}$ and the propagation constant $k_d = k\sqrt{\varepsilon_r}$, where ε_r is the relative dielectric permittivity of the medium (with relative magnetic permeability $\mu_r = 1$).

For the sake of simplicity, the structure is studied considering E_z polarization, and however, generalization to H_z polarization or skew incident case is possible and it doubles the equations. In Fig. 1, the origin O of coordinate axes is located at the edge of the corner of the dielectric half-layer fully immersed in free space. In this work, we use both Cartesian and polar coordinate systems centered in O: (x, y, z) and (ρ, φ, z).

Let us divide the problem into three homogeneous regions of simple canonical shapes. The half-space $y > 0$ constitutes region A in free space, while regions 1 and 2 are half-layers of thickness d, respectively, made by free space and dielectric material. Regions 1 and 2, respectively, occupy $x > 0$ $-d < y < 0$ and $x < 0$ $-d < y < 0$. Both half-layers are terminated by the PEC plane at $y = -d$.

Time harmonic fields are assumed with a time dependence specified by $e^{+j\omega t}$, which is omitted, and at the E_z polarization, the nonnull field components $E_z(x, y)$, $H_x(x, y)$, $H_y(x, y)$ are independent of z and are governed by the wave equation

$$\partial^2 E_z/\partial x^2 + \partial^2 E_z/\partial y^2 + k^2 E_z = 0 \tag{1}$$

where k is the propagation constant of free space (regions A and 1) and it is substituted by $k_d = k_o\sqrt{\varepsilon_r}$ in the dielectric medium (region 2).

With reference to Fig. 1, the boundary conditions of the problem among the three regions are given as follows.

1) $E_z(x, y = -d) = 0$ (PEC condition).
2) Continuity of E_z, H_y at the free space/dielectric interface $x = 0$, $-d < y < 0$ between regions 1 and 2, i.e., $E_z(x = 0_-, y) = E_z(x = 0_+, y)$, $H_y(x = 0_-, y) = H_y(x = 0_+, y)$.

3) Continuity of E_z, H_x at the free space/dielectric interface $y = 0$ between region A and regions 1 and 2, i.e., $E_z(x, y = 0_-) = E_z(x, y = 0_+)$, $H_x(x, y = 0_-) = H_x(x, y = 0_+)$.

As $\rho \to 0$ near the edge at point O, $E_z(\rho, \varphi)$ remains finite (Meixner's edge condition [45]): $E_z(\rho, \varphi) = M_0 + O(\rho^m)$ with constant M_0 and $m > 0$. The same singularity behavior with different singularity coefficients m holds at point $(x, y) = (-d, 0)$ due to the presence of the PEC surface in contact to a right-angled dielectric corner [46].

In all the regions, the following radiation condition holds while assuming small vanishing losses: $|E_z(\rho, \varphi) - E_z^{GO}(\rho, \varphi)| \leq e^{-a\rho}$ with $a > 0$, where E_z^{GO} is the total geometrical optics (GO) components of the total field E_z. The uniqueness of the solution of the wave equation is a consequence of the imposition of the boundary conditions, the edge condition, and the radiation conditions (uniqueness theorem, see, for instance, [47]).

The formulation of the problem in the spectral domain is based on the definition of bilateral and unilateral Laplace transforms. The bilateral Laplace transform of the E_z- and H_x-field components is

$$\begin{cases} v(\eta, y) = \displaystyle\int_{-\infty}^{\infty} E_z(x, y) e^{j\eta x} dx \\ i(\eta, y) = \displaystyle\int_{-\infty}^{\infty} H_x(x, y) e^{j\eta x} dx \end{cases} \tag{2}$$

while the unilateral Laplace transforms of E_z- and H_x-field components are, respectively, for $x > 0$

$$\begin{cases} \tilde{E}_{z+}(\eta, y) = \displaystyle\int_{0}^{\infty} E_z(x, y) e^{j\eta x} dx \\ \tilde{H}_{x+}(\eta, y) = \displaystyle\int_{0}^{\infty} H_x(x, y) e^{j\eta x} dx \end{cases} \tag{3}$$

and for $x < 0$

$$\begin{cases} \tilde{E}_{z-}(\eta, y) = \displaystyle\int_{-\infty}^{0} E_z(x, y) e^{j\eta x} dx \\ \tilde{H}_{x-}(\eta, y) = \displaystyle\int_{-\infty}^{0} H_x(x, y) e^{j\eta x} dx. \end{cases} \tag{4}$$

We also define the specialized unilateral transforms

$$\begin{cases} V_+(\eta) = \tilde{E}_{z+}(\eta, 0), & I_+(\eta) = \tilde{H}_{x+}(\eta, 0) \\ V_-(\eta) = \tilde{E}_{z-}(\eta, 0), & I_-(\eta) = \tilde{H}_{x-}(\eta, 0) \end{cases} \tag{5}$$

as axial spectra, and in the following, we apply also the notations $V_{\pi+}(\eta) = V_-(-\eta)$ and $I_{\pi+}(\eta) = -I_-(-\eta)$ that takes origin from the definition of radial Laplace transforms in angular regions [31] for $\varphi = \pi$ $(\sigma = \eta)$:

$$\begin{cases} V_{\varphi+}(\sigma) = \displaystyle\int_{0}^{\infty} E_z(\rho, \varphi) e^{j\sigma\rho} d\rho \\ I_{\varphi+}(\sigma) = \displaystyle\int_{0}^{\infty} H_\rho(\rho, \varphi) e^{j\sigma\rho} d\rho. \end{cases} \tag{6}$$

We note that for $y = 0$

$$\begin{cases} v(\eta, y = 0) = V_+(\eta) + V_-(\eta) = V_+(\eta) + V_{\pi+}(-\eta) \\ i(\eta, y = 0) = I_+(\eta) + I_-(\eta) = I_+(\eta) - I_{\pi+}(-\eta). \end{cases} \tag{7}$$

The quantities defined in (3) and (4) are, respectively, plus (+) and minus (−) functions useful for WH formulations, and $V_{\pi+}(\eta)$ and $I_{\pi+}(\eta)$ are plus functions related to the minus functions $V_-(\eta)$ and $I_-(\eta)$, respectively. Plus (minus) functions are analytic functions that are regular in an upper (lower) half-plane $Im[\eta] > Im[\eta_{up}]$ $(Im[\eta] < Im[\eta_{lo}])$ and goes to zero at infinity as Laplace transforms. The + (−) functions are nonstandard (ns), if $Im[\eta_{up}] > 0$ $(Im[\eta_{lo}] < 0)$. As commonly used in the WH method, we assume small vanishing losses to avoid the presence of singularities (as plane wave poles) in the real axis of the spectral plane η: $k = k_r - jk_i$, where $k_r, k_i > 0$ and $k_i \ll k_r$ (extension to highly lossy media is straightforward). Moreover, nonstandard singularities are due only to sources. For example, with plane wave illumination, only GO contributions generate these singularities. In particular, we note that the locations of singularities either GO or structural (such as surface and leaky wave poles) are related to the x-direction of propagation. Let us consider an E_z plane wave incident on the structure with azimuthal direction $\varphi = \varphi_o$

$$E_z^i(\rho, \varphi) = E_o e^{jk\rho\cos(\varphi - \varphi_o)}. \tag{8}$$

The plus unilateral Laplace transform (3) of (8) is

$$V_+^i(\eta) = \int_0^{\infty} E_z^i(x, y = 0) e^{j\eta x} dx = \frac{jE_o}{\eta - \eta_o} \tag{9}$$

with a pole $\eta_o = -k\cos(\varphi_o)$ whose location in η complex plane depends on the incident angle φ_o (i.e., η_o is in the 2nd or 4th quadrant along the segment that connects k to $-k$). Therefore, if $0 < \varphi_o < \pi/2$, then η_o lies in the 2nd quadrant of the complex plane η, while if $\pi/2 < \varphi_o < \pi$, then η_o lies in the 4th quadrant. In the second case, we have a standard plus function $V_+^i(\eta)$ since it is regular in the upper half-plane of the complex plane η. On the contrary, in the first case, $V_+^i(\eta)$ is a nonstandard plus function since the pole η_o is located in the upper half-plane of the complex plane η. In general, each field component (GO, surface wave, and leaky waves) is related to a singularity on the spectra (2)–(7) that lies in the η complex plane, defining the regularity region of the spectral quantities. We note that poles on the spectra derive from the kernel singularities or field components with infinite geometrical support (since Laplace transforms of quantities with finite support yield entire functions). For example, for what concern GO plane waves, we generalize (8) to

$$E_z^{go}(\rho, \varphi) = E_{go} e^{jk\rho\cos(\varphi - \varphi_{go})} \tag{10}$$

where φ_{go} (φ_{GO}) is the azimuthal direction of the wave with the lower case (upper case) subscripts go (GO) if referred to as an ingoing (outgoing) wave toward (from) the origin O of the reference system, and thus, $\varphi_{GO} = \varphi_{go} \pm \pi$. It yields that the spectrum of the plus unilateral Laplace transform (3) of (10) contains a pole $\eta_{go} = -k\cos(\varphi_{go})$ whose location in η complex plane depends on the angle φ_{go}.

One of the basic mathematical operations to implement the WH technique is the additive decomposition of an arbitrary analytic function into plus and minus components. While considering an arbitrary complex function $F(\eta)$, we obtain its decomposition in standard plus and minus components, i.e., $F(\eta) = F_+(\eta) + F_-(\eta)$, by applying the Cauchy decomposition formula [25]

$$\begin{aligned} F_+(\eta) &= \frac{1}{2\pi j} \int_{\gamma_1} \frac{F(\eta')}{\eta' - \eta} d\eta' \\ &= \frac{1}{2} F(\eta) + \frac{PV}{2\pi j} \int_{-\infty}^{+\infty} \frac{F(\eta')}{\eta' - \eta} d\eta \\ F_-(\eta) &= -\frac{1}{2\pi j} \int_{\gamma_2} \frac{F(\eta')}{\eta' - \eta} d\eta' \end{aligned}$$

$$= \frac{1}{2}F(\eta) - \frac{PV}{2\pi j}\int_{-\infty}^{+\infty}\frac{F(\eta')}{\eta'-\eta}d\eta' \qquad (11)$$

with $\eta \in \mathbb{R}$ where PV denotes the principal value and γ_1 and γ_2 are, respectively, the *smile* and the *frown* integration line in the η-plane [20], [21], [49], i.e., the real axis of η'-plane indented at $\eta' = \eta$ with a small semicircumference, respectively, in the lower and in the upper half-plane.

In Section V, we extensively apply the following generalized Cauchy decomposition formula [21], [48] in the presence of possible nonstandard singularities (offending singularities in the regularity half-plane) in general plus/minus functions:

$$\begin{aligned}
\frac{1}{2\pi j}\int_{\gamma_1}\frac{F_+(\eta')}{\eta'-\eta}d\eta' &= F_+(\eta) - F_+^{ns}(\eta)\\
\frac{1}{2\pi j}\int_{\gamma_2}\frac{F_+(\eta')}{\eta'-\eta}d\eta' &= -F_+^{ns}(\eta)\\
\frac{1}{2\pi j}\int_{\gamma_2}\frac{F_-(\eta')}{\eta'-\eta}d\eta' &= -F_-(\eta) + F_-^{ns}(\eta)\\
\frac{1}{2\pi j}\int_{\gamma_1}\frac{F_-(\eta')}{\eta'-\eta}d\eta' &= F_-^{ns}(\eta)
\end{aligned} \qquad (12)$$

for $\eta \in \mathbb{R}$, where $F_\pm^{ns}(\eta)$ are nonstandard parts of $F_\pm(\eta)$, i.e., $F_\pm(\eta) = F_\pm^{s}(\eta) + F_\pm^{ns}(\eta)$ in which $F_\pm^{s}(\eta)$ are instead the standard parts. The decomposition formula (12) is fundamental for the application of the Fredholm factorization method [20], [21], which reduces the system of spectral WH equations to integral representations of second kind with compact kernels by eliminating one kind of unknowns (plus or minus). As the procedure reported in Section V, we select the elimination of the minus unknowns for the solution of WH equations.

III. Incomplete WH Spectral Formulation of the Problem

With reference to Fig. 1, we formulate the problem in the spectral domain for the three regions (A, 1, and 2), starting from the wave equation (1) with the application of the Laplace transforms, the constitutive relations, and the boundary conditions reported in Section II.

A. Region A: Homogenous Half-Space

In the homogeneous half-space region A, we apply the spectral representation of planar stratified regions as reported in classical literature, see [21], [50], [51], and references therein. The transversalization of Maxwell's equations with respect to y at the E_z polarization yields the following equivalent transmission line (TL) equations in terms of bilateral Laplace transforms (2):

$$\begin{cases} -\dfrac{dv(\eta,y)}{dx} = j\xi Z_c i(\eta,y) \\ -\dfrac{di(\eta,y)}{dx} = j\xi Y_c v(\eta,y) \end{cases} \qquad (13)$$

where $\xi = \xi(\eta) = \sqrt{k^2-\eta^2}$ (omitting η dependence in the following) is the spectral propagation constant and

$$Z_c = Z_c(\eta) = 1/Y_c = 1/Y_c(\eta) = kZ_o/\xi \qquad (14)$$

is the spectral characteristic impedance of the TL along y. Since $k^2 = \eta^2+\xi^2$, $\xi(\eta)$ is a multivalued function of η. In the following, we assume as proper sheet of $\xi(\eta)$ the one with $\xi(0) = k$ and as branch lines the classical line $Im[\xi(\eta)] = 0$ (see in practical engineering estimations [50, Ch. 5.3b]) or the vertical lines ($Re[\eta] = Re[k]$, $Im[\eta] < Im[k]$) and ($Re[\eta] = Re[-k]$, $Im[\eta] > Im[-k]$).

For an indefinite half medium/TL locates at $y > 0$, we get the admittance model

$$i(\eta,0) = Y_c(\eta)v(\eta,0) \qquad (15)$$

that can be reformulated in terms of unilateral Laplace transforms (7), i.e., WH unknowns

$$I_+(\eta) - I_{\pi+}(-\eta) = Y_c(\eta)\big[V_+(\eta) + V_{\pi+}(-\eta)\big]. \qquad (16)$$

B. Regions 1 and 2: Grounded Half-Layer

In this section, we present an original representation of regions 1 and 2 (Fig. 1) based on the solution of partial differential problems with the application of a revisited characteristic Green's function procedure in the spectral domain.

Let us consider region 1 to develop the theory in detail and then extrapolate equations for region 2. As reported in Section II, we assume for illustrative purposes that region 1 is filled by vacuum. By applying the unilateral right Laplace transforms (3) to the wave equation (1), we obtain the ordinary differential equation in y

$$\left(\frac{d^2}{dy^2} + \xi^2\right)\tilde{E}_{z+}(\eta,y) = f_1(\eta,y) \qquad (17)$$

where the initial conditions of $E_z(x,y)$ at $x = 0_+$ yields

$$f_1(\eta,y) = -j\eta E_z(0_+,y) + j\omega\mu_o H_y(0_+,y) \qquad (18)$$

after the application of Maxwell's equation in the second term. Equation (17) is a differential equations of second order in y with forcing function $f_1(\eta,y)$ and boundary conditions as reported in Section II with points 1) and 3). As in classical literature, the solution is obtainable as sum of a particular integral with a complementary function, which is a linear combination of homogeneous equation solutions.

A general method to represent the solution is reported in [43] where the characteristic Green's function procedure to represent the particular integral is generalized and applied to the unmixed nonhomogeneous boundary condition problem. In fact, it is possible to build a Green's function starting from arbitrary solutions of the homogeneous equation ignoring the boundary conditions of the problem at first. Green's function needs to satisfy three conditions: 1) to be a continuous function at $y = y'$; 2) to have a derivative with jump at $y = y'$; and 3) to be solution of the related homogeneous equations. The solution of the problem is then constituted by the combination of the particular integral with the homogeneous portion of the solution (complementary function) whose arbitrary coefficients are uniquely defined by the imposition of boundary conditions.

To address the problem, we here select from the set of arbitrary homogeneous solutions of (17)

$$\begin{cases} \overleftarrow{\varphi}_{1\eta}(y) = \sin(\xi(y+d)) \\ \vec{\varphi}_{1\eta}(y) = \cos(\xi y) \end{cases} \qquad (19)$$

where $\overleftarrow{\varphi}_{1\eta}(y)$ satisfies the physical boundary condition at $y = -d$ (PEC), while $\vec{\varphi}_{1\eta}(y)$ satisfies a perfectly magnetically conducting (PMC) boundary condition at $y = 0$ that is not directly related to any physical property of the problem. In fact, while the boundary condition 1) of Section II (PEC) holds at $y = -d$, at $y = 0$, we have the continuity boundary

condition 3). According to [43] and (19), Green's function takes the form

$$g_{1\eta}(y,y') = \frac{\overleftarrow{\varphi}_{1\eta}(y_<)\vec{\varphi}_{1\eta}(y_>)}{W_r\left[\overleftarrow{\varphi}_{1\eta}(y_<),\vec{\varphi}_{1\eta}(y_>)\right]} = \frac{\cos(\xi y_>)\sin(\xi(y_<+d))}{-\xi\cos(\xi d)} \tag{20}$$

where $W_r[\overleftarrow{\varphi}_{1\eta}(y),\vec{\varphi}_{1\eta}(y)]$ is the Wronskian of the two functions $\overleftarrow{\varphi}_{1\eta}(y)$ and $\vec{\varphi}_{1\eta}(y)$ and $y_<$ and $y_>$ denote, respectively, the lesser and the greater of quantities y and y'. The solution of (17) is therefore

$$\tilde{E}_{z+}(\eta,y) = \int_{-d}^{0} g_{1\eta}(y,y')f_1(\eta,y')dy' + A_1(\eta)\overleftarrow{\varphi}_{1\eta}(y) + B_1(\eta)\vec{\varphi}_{1\eta}(y) \tag{21}$$

with arbitrary coefficients $A_1(\eta)$ and $B_1(\eta)$. Following the classification of [43], our problem is with unmixed nonhomogeneous boundary condition due to the $y=0$ interface, while $y=-d$ is a homogeneous boundary condition (PEC). For this reason, by selecting (19) and imposing the physical boundary condition at $y=-d$ on (21), we get $B(\eta)=0$, yielding

$$\tilde{E}_{z+}(\eta,y) = \int_{-d}^{y}\frac{\cos(\xi y)\sin\left(\xi\left(y'+d\right)\right)}{-\xi\cos(\xi d)}f_1(\eta,y')dy' + \int_{y}^{0}\frac{\cos\left(\xi y'\right)\sin(\xi(y+d))}{-\xi\cos(\xi d)}f_1(\eta,y')dy' + A_1(\eta)\sin(\xi(y+d)) \tag{22}$$

as $\tilde{E}_{z+}(\eta,-d)=0$.

Now, in order to explicit the continuity of fields at $y=0$ and we determine $A_1(\eta)$ in terms of the continuous field. Putting $y=0$ in (22), we get

$$\tilde{E}_{z+}(\eta,0) = \int_{-d}^{0}\frac{\sin\left(\xi\left(y'+d\right)\right)}{-\xi\cos(\xi d)}f_1(\eta,y')dy' + A_1(\eta)\sin(\xi d) \tag{23}$$

where $\tilde{E}_{z+}(\eta,0)=V_+(\eta)$ as defined in (5). The application of Maxwell's equation to (22) and the imposition of $y=0$ yield

$$\tilde{H}_{x+}(\eta,0) = -\frac{\xi}{jkZ_o}A_1(\eta)\cos(\xi d) \tag{24}$$

where $\tilde{H}_{x+}(\eta,0)=I_+(\eta)$ (5) thus

$$A_1(\eta) = -\left(\frac{\xi\cos(\xi d)}{jkZ_o}\right)^{-1}I_+(\alpha). \tag{25}$$

Substituting (25) into (23), after some mathematical manipulation, we get the following spectral representation:

$$\int_{-d}^{0}\frac{\sin\left(\xi\left(y'+d\right)\right)}{-jkZ_o\sin(\xi d)}f_1(\eta,y')dy' - I_+(\eta) = Y_{d1}(\eta)V_+(\eta) \tag{26}$$

where

$$Y_{d1}(\eta) = \frac{-j\,\xi}{k\,Z_o}\cot(\xi d). \tag{27}$$

We note that the presence of $Y_{d1}(\eta)$ in (26) defines an admittance relation between $V_+(\eta)$ and $I_+(\eta)$ as in a layer of thickness d terminated by a PEC boundary. However, the equation also contains an integral unknown term related to the boundary condition 2) of Section II (interface at $x=0$) through the definition of $f_1(\eta,y)$ (18). For this reason, (26) is called an incomplete WH equation since it needs some more specifications to become an explicit representation.

We recall that the selection of homogeneous equation solutions for the construction of Green's function (particular integral) and the complementary function are arbitrary and the imposition of boundary conditions appropriately selects the arbitrary coefficients: for instance, (26) can be derived by selecting as solutions of the homogeneous equations the ones with PMC fictitious boundary conditions at $y=0,-d$.

While analyzing region 2, in the following, we assume for illustrative purposes that it is constituted of dielectric, and however, the medium can be generalized as reported in Section I. We repeat the same methodology used for region 1 by applying, in this case, the unilateral left Laplace transforms (4) to the wave equation (1). It yields the ordinary differential equation in y

$$\left(\frac{d^2}{dy^2}+\xi_d^2\right)\tilde{E}_{z-}(\eta,y) = f_2(\eta,y) \tag{28}$$

where $\xi_d=\xi_d(\eta)=\sqrt{k_d^2-\eta^2}$ is the spectral propagation constant and the initial conditions of $E_z(x,y)$ at $x=0_-$ yield

$$f_2(\eta,y) = j\eta E_z(0_-,y) - j\omega\mu_o H_y(0_-,y). \tag{29}$$

Since ξ_d of region 2 is a multivalued function of η, in the following, we extend the analytical assumptions reported for ξ of region 1 to ξ_d according to the due differences between the two media.

Again, (28) is a differential equation of second order with forcing function $f_2(\eta,y)$ and boundary conditions as reported in Section II with points 1) and 3). Following the same procedure described for region 1, we select from the set of arbitrary homogeneous solutions

$$\begin{cases}\overleftarrow{\varphi}_{2\eta}(y)=\sin(\xi_d(y+d))\\ \vec{\varphi}_{2\eta}(y)=\cos(\xi_d y)\end{cases} \tag{30}$$

where $\overleftarrow{\varphi}_{2\eta}(y)$ satisfies the physical PEC boundary condition at $y=-d$, while $(\vec{\varphi}_{2\eta}(y)$ satisfies a fictitious PMC boundary condition at $y=0$. Green's function of region 2 takes the form

$$g_{2\eta}(y,y') = \frac{\cos(\xi_d y_>)\sin(\xi_d(y_<+d))}{-\xi_d\cos(\xi_d d)}. \tag{31}$$

The solution of (28) is therefore

$$\tilde{E}_{z-}(\eta,y) = \int_{-d}^{0}g_{2\eta}(y,y')f_2(\eta,y')dy' + A_2(\eta)\overleftarrow{\varphi}_{2\eta}(y) + B_2(\eta)\vec{\varphi}_{2\eta}(y) \tag{32}$$

with arbitrary coefficients $A_2(\eta)$ and $B_2(\eta)$.

By imposing and imposing the PEC physical boundary condition at $y=-d$, we get $B_2(\eta)=0$, and thus,

$$\tilde{E}_{z-}(\eta,y) = \int_{-d}^{y}\frac{\cos(\xi_d y)\sin\left(\xi_d\left(y'+d\right)\right)}{-\xi_d\cos(\xi_d d)}f_2(\eta,y')dy' + \int_{y}^{0}\frac{\cos\left(\xi_d y'\right)\sin(\xi_d(y+d))}{-\xi_d\cos(\xi_d d)}f_2(\eta,y')dy' + A_2(\eta)\sin(\xi(y+d)) \tag{33}$$

as $\tilde{E}_{z-}(\eta,-d)=0$. Note that $\tilde{E}_{z-}(\eta,0)=V_-(\eta)=V_{\pi+}(-\eta)$ (5). By applying Maxwell's equatiosn to (33), at $y=0$, we get

$$A_2(\eta) = -\left(\frac{\xi_d\cos(\xi_d d)}{jkZ_o}\right)^{-1}I_+(\alpha) \tag{34}$$

where $\tilde{H}_{x-}(\eta,0) = I_-(\eta) = -I_{\pi+}(-\eta)$ (5).

Substituting (34) into (33), after some mathematical manipulation, we get at $y=0$ the following spectral representation:

$$\int_{-d}^{0} \frac{\sin\big(\xi_d\big(y'+d\big)\big)}{-jkZ_o\sin(\xi_d d)} f_2(\eta,y')dy' + I_{\pi+}(-\eta) = Y_{d2}(\eta)V_{\pi+}(-\eta) \quad (35)$$

where

$$Y_{d2}(\eta) = \frac{-j\,\xi_d}{k\,Z_o}\cot(\xi_d d). \quad (36)$$

From (35), we finally get the incomplete WH equation for region 2

$$\int_{-d}^{0} \frac{\sin\big(\xi_d\big(y'+d\big)\big)}{-jkZ_o\sin(\xi_d d)} f_2(-\eta,y')dy' + I_{\pi+}(\eta) = Y_{d2}(\eta)V_{\pi+}(\eta) \quad (37)$$

that defines an admittance relation.

IV. Complete WH Equations

The WH formulation of the problem given in Section III provides a set of WH coupled equations reported in (16), (26), and (35). While (16) is an explicit expression in terms of spectral WH unknowns, (26) and (35) present incompleteness due to the presence of coupling integral terms related to the boundary condition at $x=0$, $-d<y<0$. In fact, we call incomplete equations the WH equations that contain spectral unknowns not explicitly expressed in terms of the spectral WH unknowns. In this section, we eliminate incompleteness from our WH formulation.

With reference to region 1, the integral term in (26) can be represented through (18) as

$$-\frac{\int_{-d}^{0}\sin\big(\xi\big(y'+d\big)\big)f_1(\eta,y')dy'}{jkZ_o\sin(\xi d)} = p_0(\xi)+\eta p_1(\xi) \quad (38)$$

with

$$p_0(\xi) = -\frac{\int_{-d}^{0}\sin\big(\xi\big(y'+d\big)\big)H_y(0_+,y')dy'}{\sin(\xi d)}$$
$$p_1(\xi) = \frac{\int_{-d}^{0}\sin\big(\xi\big(y'+d\big)\big)E_z(0_+,y')dy'}{kZ_o\sin(\xi d)}. \quad (39)$$

Since $p_{0,1}(\xi)$ are meromorphic function of ξ with poles at $\sin(\xi d)=0$, i.e., $\xi_n = (n\pi/d)$, $n\in\mathbb{N}$, we have after some mathematical manipulations on the Mittag–Leffler representations in partial fractions of (39)

$$p_0(\xi) = \sum_{n=1}^{\infty}\frac{a_n}{\xi^2-\xi_n^2} = -\sum_{n=1}^{\infty}\frac{a_n}{\eta^2-\eta_n^2}$$
$$p_1(\xi) = -\sum_{n=1}^{\infty}\frac{b_n}{\eta^2-\eta_n^2} \quad (40)$$

with $\eta_n^2 = k^2-(n\pi/d)^2$, $n\in\mathbb{N}$ and unknown coefficients a_n and b_n. Substituting (38)–(40) in (26), it yields

$$-\sum_{n=1}^{\infty}\frac{a_n}{\eta^2-\eta_n^2} - \eta\sum_{n=1}^{\infty}\frac{b_n}{\eta^2-\eta_n^2} - I_+(\eta) = Y_{d1}(\eta)V_+(\eta). \quad (41)$$

We now observe that due to definitions (18) and (29), in the case of dielectric medium in region 2, we have

$$f_2(-\eta,y) = -f_1(-\eta,y). \quad (42)$$

Therefore, the integral term of (37) in region 2 can be represented as

$$-\frac{\int_{-d}^{0}\sin\big(\xi_d\big(y'+d\big)\big)f_2(-\eta,y')dy'}{jkZ_o\sin(\xi_d d)} = -p_0(\xi_d)+\eta p_1(\xi_d). \quad (43)$$

The meromorphic functions $p_{0,1}(\xi_d)$ are represented as

$$p_0(\xi_d) = \sum_{n=1}^{\infty}\frac{a_n}{\xi_d^2-\xi_{dn}^2} = -\sum_{n=1}^{\infty}\frac{a_n}{\eta^2-\chi_n^2}$$
$$p_1(\xi_d) = -\sum_{n=1}^{\infty}\frac{b_n}{\eta^2-\chi_n^2} \quad (44)$$

with $\xi_{dn} = (n\pi/d)$, $\chi_n^2 = k_d^2-(n\pi/d)^2$, $n\in\mathbb{N}$, and unknown coefficients a_n and b_n. Substituting (43) and (44) into (37), it yields

$$\sum_{n=1}^{\infty}\frac{a_n}{\eta^2-\chi_n^2} - \eta\sum_{n=1}^{\infty}\frac{b_n}{\eta^2-\chi_n^2} + I_{\pi+}(\eta) = Y_{d2}(\eta)V_{\pi+}(\eta). \quad (45)$$

We observe that η_n and ξ_n in (41) and (45), respectively, represent pseudo-modes of the equivalent parallel PEC plate waveguides filled by vacuum and dielectric material. Later, we will demonstrate that these nonphysical modes will not contribute to the spectral solutions. Equations (41) and (45) still represent a set of incomplete WH equations, and however, we can exploit the regularity properties of plus WH unknowns in the upper half-plane of the complex variable η estimating the residue of (41) at $\eta=-\eta_n$ and of (45) at $\eta=-\chi_n$ (points located in the upper half-complex plane). It yields the following set of equations in a_n and b_n:

$$\begin{cases} \dfrac{a_n}{2\xi_n} - \dfrac{b_n}{2} = -\dfrac{j\pi^2n^2}{d^3kZ_o\eta_n}V_+(-\eta_n) \\ -\dfrac{a_n}{2\chi_n} - \dfrac{b_n}{2} = -\dfrac{j\pi^2n^2}{d^3kZ_o\chi_n}V_{\pi+}(-\chi_n) \end{cases} \quad (46)$$

that allows to represent a_n and b_n in terms of samples of WH unknowns

$$\begin{cases} a_n = -\dfrac{2j\pi^2n^2\big[\chi_nV_+(-\eta_n)-\eta_nV_{\pi+}(-\chi_n)\big]}{d^3kZ_o(\eta_n+\chi_n)} \\ b_n = \dfrac{2j\pi^2n^2\big[V_+(-\eta_n)+V_{\pi+}(-\chi_n)\big]}{d^3kZ_o(\eta_n+\chi_n)} \end{cases} \quad (47)$$

removing the incompleteness in WH formulation (41) and (45) that together with already explicit (16) model the problem.

V. Fredholm Factorization of WH Formulation

In this section, we apply a modified version of Fredholm factorization method to the WH formulation (16), (41), and (45) completed with explicit a_n and b_n expressions reported at (47) avoiding recursive algorithm as proposed in [31] for a different but mathematically similar problem.

This methodology directly provides a system of explicit FIEs in terms of one kind of spectral WH unknowns through the application of Cauchy integral representations (12). In the present application, we privilege plus unknowns by removing minus ones.

We observe that the explicitness of the formulation is a great advantage with respect to an approximate solution based on infinite linear system of equations that require a multistep

analysis for convergence as often reported in the WH literature [15], [17], [18], [29].

We observe that the application of Fredholm factorization allows to get regularized integral representations with compact kernels. Finally, the semianalytical solution of the system of FIEs provides the true spectra of field components from which we extract by asymptotics physical/engineering phenomena excited by the structure like in closed-form analytical solutions.

A. Application to Region A

In region A, the explicit WH equation (16) holds. The Fredholm factorization is here applied to the original version of (16) and to (16) while substituting η with $-\eta$. This manipulation of the equations allows to get integral representations for both + and $\pi+$ unknowns, respectively $[V_+(\eta), I_+(\eta)]$ and $[V_{\pi+}(\eta), I_{\pi+}(\eta)]$, by working with Fredholm factorization that removes minus unknowns. Let us first consider the original version of (16). The application of the smile contour γ_1 integration to the left-hand side (LHS) of (16) yields

$$\frac{1}{2\pi j}\int_{\gamma_1}\frac{I_+(\eta')-I_{\pi+}(-\eta')}{\eta'-\eta}d\eta' = I_+(\eta)-I_+^{ns}(\eta)-I_{\pi+}^{ns}(-\eta) \tag{48}$$

according to (12). For the right-hand side (RHS), we get

$$\begin{aligned}&\frac{1}{2\pi j}\int_{\gamma_1}\frac{Y_c(\eta')[V_+(\eta')+V_{\pi+}(-\eta')]}{\eta'-\eta}d\eta'\\&= Y_c(\eta)V_+(\eta)+\frac{1}{2\pi j}\int_{-\infty}^{\infty}\frac{[Y_c(\eta')-Y_c(\eta)]V_+(\eta')]}{\eta'-\eta}d\eta'\\&\quad -Y_c(\eta)V_+^{ns}(\eta)+\frac{1}{2\pi j}\int_{-\infty}^{\infty}\frac{[Y_c(\eta)-Y_c(\eta')]V_{\pi+}(\eta')}{\eta'+\eta}d\eta'\\&\quad +Y_c(\eta)V_{\pi+}^{ns}(-\eta)\end{aligned} \tag{49}$$

where we have added and subtracted

$$\frac{1}{2\pi j}\int_{\gamma_2}\frac{Y_c(\eta)V_+(\eta')}{\eta'-\eta}d\eta'+\frac{1}{2\pi j}\int_{\gamma_1}\frac{Y_c(\eta)V_{\pi+}(-\eta')}{\eta'-\eta}d\eta' \tag{50}$$

and applied (11) and (12). In fact, we have

$$\begin{aligned}&\frac{1}{2\pi j}\int_{\gamma_1}\frac{Y_c(\eta')V_+(\eta')}{\eta'-\eta}d\eta'-\frac{1}{2\pi j}\int_{\gamma_2}\frac{Y_c(\eta)V_+(\eta')}{\eta'-\eta}d\eta'\\&= \frac{PV}{2\pi j}\int_{-\infty}^{\infty}\frac{Y_c(\eta')V_+(\eta')}{\eta'-\eta}d\eta'+\frac{1}{2}Y_c(\eta)V_+(\eta)+\\&\quad -\frac{PV}{2\pi j}\int_{-\infty}^{\infty}\frac{Y_c(\eta)V_+(\eta')}{\eta'-\eta}d\eta'+\frac{1}{2}Y_c(\eta)[V_+(\eta)]\\&= Y_c(\eta)V_+(\eta)+\frac{1}{2\pi j}\int_{-\infty}^{\infty}\frac{[Y_c(\eta')-Y_c(\eta)]V_+(\eta')}{\eta'-\eta}d\eta'\end{aligned} \tag{51}$$

$$\frac{1}{2\pi j}\int_{\gamma_2}\frac{Y_c(\eta)V_+(\eta')}{\eta'-\eta}d\eta' = -Y_c(\eta)V_+^{ns}(\eta) \tag{52}$$

$$\begin{aligned}&\frac{1}{2\pi j}\int_{\gamma_1}\frac{Y_c(\eta')V_{\pi+}(-\eta')}{\eta'-\eta}d\eta'-\frac{1}{2\pi j}\int_{\gamma_1}\frac{Y_c(\eta)V_{\pi+}(-\eta')}{\eta'-\eta}d\eta'\\&= \frac{1}{2\pi j}\int_{-\infty}^{\infty}\frac{[Y_c(\eta')-Y_c(\eta)]V_{\pi+}(-\eta')}{\eta'-\eta}d\eta'\\&= \frac{1}{2\pi j}\int_{-\infty}^{\infty}\frac{[Y_c(\eta)-Y_c(\eta')]V_{\pi+}(\eta')}{\eta'+\eta}d\eta'\end{aligned} \tag{53}$$

$$\frac{1}{2\pi j}\int_{\gamma_1}\frac{Y_c(\eta)V_{\pi+}(-\eta')}{\eta'-\eta}d\eta' = Y_c(\eta)V_{\pi+}^{ns}(-\eta) \tag{54}$$

recalling that a plus function in η evaluated in $-\eta$ is a minus function in η. Considering the γ_1 integration on (16), combining (48) with (49), we get the integral representation (55) that relates plus unknowns with

$$\begin{aligned}&-I_+(\eta)\\&= -Y_c(\eta)V_+(\eta)-\frac{1}{2\pi j}\int_{-\infty}^{\infty}\frac{[Y_c(\eta')-Y_c(\eta)]V_+(\eta')}{\eta'-\eta}d\eta'\\&\quad -\frac{1}{2\pi j}\int_{-\infty}^{\infty}\frac{[Y_c(\eta)-Y_c(\eta')]V_{\pi+}(\eta')}{\eta'+\eta}d\eta'-I_c(\eta)\end{aligned} \tag{55}$$

$$I_c(\eta) = I_+^{ns}(\eta)-Y_c(\eta)V_+^{ns}(\eta)+Y_c(\eta)V_{\pi+}^{ns}(-\eta)+I_{\pi+}^{ns}(-\eta). \tag{56}$$

Applying the same procedure to (16) while substituting η with $-\eta$, we get (57), which is a second integral representation that relates plus unknowns with

$$\begin{aligned}&I_{\pi+}(\eta)\\&= -Y_c(\eta)V_{\pi+}(\eta)-\frac{1}{2\pi j}\int_{-\infty}^{\infty}\frac{[Y_c(\eta')-Y_c(\eta)]V_{\pi+}(\eta')}{\eta'-\eta}\\&\quad -\frac{1}{2\pi j}\int_{-\infty}^{\infty}\frac{[Y_c(\eta)-Y_c(\eta')]V_+(\eta')}{\eta'+\eta}d\eta'+I_{c\pi}(\eta)\end{aligned} \tag{57}$$

$$I_{c\pi}(\eta) = I_{\pi+}^{ns}(\eta)+Y_c(\eta)V_{\pi+}^{ns}(\eta)-Y_c(\eta)V_+^{ns}(-\eta)+I_+^{ns}(-\eta). \tag{58}$$

As stated in Section II, the spectra of WH unknowns can contain nonstandard (ns) offending GO components that the Fredholm factorization procedure has extracted as contribution in (55)–(57). The estimation of these contributions is reported in the Appendix.

B. Application to Regions 1 and 2

Let us consider (41) for region 1 to develop the theory in detail and then extrapolate equations for region 2 considering (45). The application of the smile contour γ_1 integration to (41) with decomposition formula (12) yields

$$\begin{aligned}&-\sum_{n=1}^{\infty}\frac{a_n+b_n\eta_n}{2\eta_n(\eta-\eta_n)}-I_+(\eta)+I_+^{ns}(\eta)\\&\qquad = \frac{1}{2\pi j}\int_{\gamma_1}\frac{Y_{d1}(\eta')V_+(\eta')}{\eta'-\eta}d\eta'.\end{aligned} \tag{59}$$

From (12), we subtract

$$Y_{d1}(\eta)\left[\frac{1}{2\pi j}\int_{\gamma_2}\frac{V_+(\eta')}{\eta'-\eta}d\eta'+V_+^{ns}(\eta)\right] = 0 \tag{60}$$

from the RHS of (59) providing

$$\begin{aligned}&\frac{1}{2\pi j}\int_{\gamma_1}\frac{Y_{d1}(\eta')V_+(\eta')}{\eta'-\eta}d\eta'\\&= Y_{d1}(\eta)V_+(\eta)+\frac{1}{2\pi j}\int_{-\infty}^{\infty}\frac{[Y_{d1}(\eta')-Y_{d1}(\eta)]V_+(\eta')}{\eta'-\eta}d\eta'\\&\quad -Y_{d1}(\eta)V_+^{ns}(\eta).\end{aligned} \tag{61}$$

Substituting (61) into (59) together with a_n and b_n (47), we get an integral representation (63) that relates plus unknowns with an implicit sampling of the spectra in points $-\eta_n$ and $-\chi_n$ located in the upper half-plane through

$$H_{11}(\eta,n) = \frac{jn^2\pi^2(\eta_n-\chi_n)}{d^3kZ_o\eta_n(\eta_n-\eta)(\eta_n+\chi_n)}$$

$$H_{12}(\eta,n)=\frac{2jn^2\pi^2}{d^3kZ_o(\eta_n-\eta)(\eta_n+\chi_n)}. \tag{62}$$

To remove this implicitness of formulation

$$\begin{aligned}&\sum_{n=1}^{\infty}[H_{11}(\eta,n)V_+(-\eta_n)+H_{12}(\eta,n)V_{\pi+}(-\chi_n)]\\&\quad-I_+(\eta)+I_+^{ns}(\eta)\\&\quad=Y_d(\eta)V_+(\eta)+\frac{1}{2\pi j}\int_{-\infty}^{\infty}\frac{[Y_{d1}(\eta')-Y_{d1}(\eta)]V_+(\eta')}{\eta'-\eta}d\eta'\\&\quad-Y_{d1}(\eta)V_+^{ns}(\eta)\end{aligned} \tag{63}$$

we resort again to the Cauchy formula (12) by substituting

$$V_+(-\eta_n)=\frac{1}{2\pi j}\int_{-\infty}^{\infty}\frac{V_+(\eta')}{\eta'+\eta_n}d\eta'+V_+^{ns}(-\eta_n). \tag{64}$$

Note that the ns spectrum sampling in (64) is known and enriches the known terms already present in (63), while the integral term increments the integral kernel.

We repeat the procedure for (45), starting from the γ_1 contour integration

$$\begin{aligned}&\sum_{n=1}^{\infty}\frac{a_n-b_n\chi_n}{2\chi_n(\eta-\chi_n)}+I_{\pi+}(\eta)-I_{\pi+}^{ns}(\eta)\\&\qquad=\frac{1}{2\pi j}\int_{\gamma_1}\frac{Y_{d2}(\eta')V_{\pi+}(\eta')}{\eta'-\eta}d\eta'.\end{aligned} \tag{65}$$

At the end of the procedure, the integral representation (66) is obtained with

$$\begin{aligned}&\sum_{n=1}^{\infty}[H_{21}(\eta,n)V_+(-\eta_n)+H_{22}(\eta,n)V_{\pi+}(-\chi_n)]\\&\quad+I_{\pi+}(\eta)-I_{\pi+}^{ns}(\eta)\\&\quad=Y_{d2}(\eta)V_{\pi+}(\eta)+\frac{1}{2\pi j}\int_{-\infty}^{\infty}\frac{[Y_{d2}(\eta')-Y_{d2}(\eta)]V_{\pi+}(\eta')}{\eta'-\eta}d\eta'\\&\quad-Y_{d2}(\eta)V_{\pi+}^{ns}(\eta)\end{aligned} \tag{66}$$

with sample spectra represented via

$$V_{\pi+}(-\chi_n)=\frac{1}{2\pi j}\int_{-\infty}^{\infty}\frac{V_{\pi+}(\eta')}{\eta'+\chi_n}d\eta'+V_{\pi+}^{ns}(-\chi_n) \tag{67}$$

and

$$\begin{aligned}H_{21}(\eta,n)&=\frac{2jn^2\pi^2}{d^3kZ_o(\chi_n-\eta)(\eta_n+\chi_n)}\\H_{22}(\eta,n)&=-\frac{jn^2\pi^2(\eta_n-\chi_n)}{d^3kZ_o\chi_n(\chi_n-\eta)(\eta_n+\chi_n)}.\end{aligned} \tag{68}$$

The estimation of ns terms is reported in the Appendix.

VI. System of FIEs and Its Solution

The integral representations (55), (57), (63), and (66) obtained in Section V through the application of a modified version of Fredholm factorization relate the current plus WH unknowns $(I_+(\eta), I_{\pi+}(\eta))$ to the voltage plus WH unknowns $[V_+(\eta), V_{\pi+}(\eta)]$. This system of equations can be interpreted as generalized equivalent network relation of Norton type, as reported in Fig. 2. In the figure, we have highlighted with generators all terms related to ns components extracted from the spectra with the Fredholm factorization procedure, while the algebraic and integral operator applied to the voltage unknowns are modeled via multiport generalized matrix admittances.

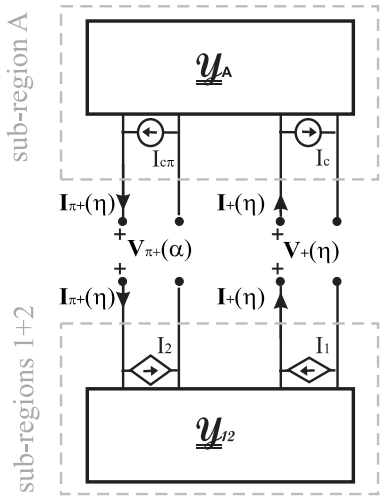

Fig. 2. Network equivalent model of integral representations (55), (57), (63), and (66). With reference to Fig. 1, the first two equations are related to region A, while the last two equations are related to regions 1 and 2.

From the system of equations, we eliminate the current plus WH unknowns $[I_+(\eta), I_{\pi+}(\eta)]$ substituting (55) into (63) and (57) into (66). It yields the system of FIEs of second kind of dimension 2

$$\begin{aligned}&Y_{t1}(\eta)V_+(\eta)\\&\quad+\frac{1}{2\pi j}\int_{-\infty}^{\infty}\left[\frac{Y_{t1}(\eta')-Y_{t1}(\eta)}{\eta'-\eta}-\sum_{n=1}^{\infty}\frac{H_{11}(\eta,n)}{\eta'+\eta_n}\right]V_+(\eta')d\eta'\\&\quad+\frac{1}{2\pi j}\int_{-\infty}^{\infty}\left[\frac{Y_c(\eta)-Y_c(\eta')}{\eta'+\eta}-\sum_{n=1}^{\infty}\frac{H_{12}(\eta,n)}{\eta'+\chi_n}\right]V_{\pi+}(\eta')d\eta'\\&=-I_{ct}(\eta)+\sum_{n=1}^{\infty}\left[H_{11}(\eta,n)V_+^{ns}(-\eta_n)+H_{12}(\eta,n)V_{\pi+}^{ns}(-\chi_n)\right]\end{aligned} \tag{69}$$

$$\begin{aligned}&Y_{t2}(\eta)V_{\pi+}(\eta)+\frac{1}{2\pi j}\\&\quad\times\int_{-\infty}^{\infty}\left[\frac{Y_{t2}(\eta')-Y_{t2}(\eta)}{\eta'-\eta}-\sum_{n=1}^{\infty}\frac{H_{22}(\eta,n)}{\eta'+\chi_n}\right]V_{\pi+}(\eta')d\eta'\\&\quad+\frac{1}{2\pi j}\int_{-\infty}^{\infty}\left[\frac{Y_c(\eta)-Y_c(\eta')}{\eta'+\eta}-\sum_{n=1}^{\infty}\frac{H_{21}(\eta,n)}{\eta'+\eta_n}\right]V_+(\eta')d\eta'\\&=I_{c\pi t}(\eta)+\sum_{n=1}^{\infty}\left[H_{21}(\eta,n)V_+^{ns}(-\eta_n)+H_{22}(\eta,n)V_{\pi+}^{ns}(-\chi_n)\right]\end{aligned} \tag{70}$$

in terms of voltage plus WH unknowns $[V_+(\eta), V_{\pi+}(\eta)]$ with sources

$$\begin{aligned}I_{ct}(\eta)&=-Y_{t1}(\eta)V_+^{ns}(\eta)+Y_c(\eta)V_{\pi+}^{ns}(-\eta)+I_{\pi+}^{ns}(-\eta)\\I_{c\pi t}(\eta)&=Y_{t2}(\eta)V_{\pi+}^{ns}(\eta)-Y_c(\eta)V_+^{ns}(-\eta)+I_+^{ns\cdot}(-\eta)\end{aligned} \tag{71}$$

where

$$\begin{aligned}Y_{t1}(\eta)&=Y_c(\eta)+Y_{d1}(\eta)=-j\frac{e^{j\xi d}\xi}{k\,Z_o\sin(\xi d)}\\Y_{t2}(\eta)&=Y_c(\eta)+Y_{d2}(\eta)=\frac{\xi}{k\,Z_o}-\frac{j\,\xi_d}{k\,Z_o}\cot(\xi_d d)\end{aligned} \tag{72}$$

using (14), (27), and (36). Note that (69) and (70) show additional terms under summations that sample the ns spectra. The application of (64) and (67) enriches the known terms

already present in the system of FIEs (69) and (70), while the integral terms increment the kernels.

The system of FIEs (69) and (70) can be written in a compact form as follows:

$$\underline{V}_p(\eta) + \frac{1}{2\pi j}\int_{-\infty}^{\infty} \underline{\underline{\tilde{M}}}(\eta,\eta')\underline{V}_p(\eta')d\eta' = \underline{\tilde{N}}(\eta) \tag{73}$$

with $\eta \in \mathbb{R}$ and where the vector $\underline{V}_p(\eta) = (V_+(\eta), V_{\pi+}(\eta))^t$, the matrix $\underline{\underline{\tilde{M}}}(\eta,\eta')$ contains the kernels explicitly reported in (69) and (70) and the vector $\underline{\tilde{N}}(\eta)$ is the vector known term on the right-hand sides. Note that (73) is a complete and explicit system of FIEs. In particular, we resort to the theory reported in [52, Appendix] inspired by [53] to demonstrate that (73) is with compact kernel considering a suitable generalized Hilbert space. Thus, simple numerical quadratures, such as sample and hold, allow to obtain approximate version of (73) from which we get an approximate solution [54]. We note that due to the presence of singularities near the integration line [in particular the branch points $\pm k(\pm k_d)$ of $\xi(\eta)(\xi_d(\eta))$], we warp the integration line (the real axis) into the path

$$B_\theta : \upsilon(u) = ue^{j\theta}, \quad u \in \mathbb{R},\ 0 < \theta < \pi/2 \tag{74}$$

to enhance the convergence of the integral equations [20]. We select B_θ since, in our problem, the singularities of the kernel and the sources are located in the 2nd and 4th quadrant (see also [55, Figs. 13 and 14], [56, §5.3, §5.4]).

Considering a limited interval of the spectra along B_θ with $u \in [-A, A]$ and discretizing (73) with step parameter h such that $A/h \in \mathbb{N}$, we get the linear system

$$\underline{V}_p(\upsilon(hj)) + \frac{h}{2\pi j}\sum_{i=-\frac{A}{h}}^{\frac{A}{h}} \underline{\underline{\tilde{M}}}(\upsilon(hj),\upsilon(hi))\underline{V}_p(\upsilon(hi))\upsilon'(hi) = \underline{\tilde{N}}(\upsilon(hj)) \tag{75}$$

with $j = -A/h, \ldots, A/h$, whose solution allows the reconstruction of an approximated $\underline{V}_p(\eta)$ through the samples $\underline{V}_p(\upsilon(hj))$

$$\underline{V}^a_p(\eta) = -\frac{h}{2\pi j}\sum_{i=-\frac{A}{h}}^{\frac{A}{h}} \underline{\underline{\tilde{M}}}(\eta,\upsilon(hi))\underline{V}_p(\upsilon(hi))\upsilon'(hi) + \underline{\tilde{N}}(\eta). \tag{76}$$

Once obtained $\underline{V}^a_p(\eta) = (V^a_+(\eta), V^a_{\pi+}(\eta))^t$, using a discretized version of (55) and (57) or (63) and (66) along the B_θ, we directly derive approximations for $I_+(\eta)$ and $I_{\pi+}(\eta)$.

VII. Physics-Engineering Parameters and Field's Components

Given the approximate spectra of $V_+(\eta), V_{\pi+}(\eta)$ and $I_+(\eta), I_{\pi+}(\eta)$ in the η-plane, we compute the electromagnetic field and physics-engineering parameters by applying asymptotics and the residue theorem. The singularities of the spectra are constituted by two sets: the nonstructural ones (due to sources) and the structural ones (due to the kernel). The nonstructural singularities are poles contained in $\underline{\tilde{N}}(\eta)$ of (76) and they are related to GO components while illuminating the structure with plane waves. Conversely, the structural singularities are poles or branch points originated from the FIE kernel $\underline{\underline{\tilde{M}}}(\eta,\upsilon(hi))$ in (76) and they are related to surface waves, leaky waves, and lateral waves when present. Furthermore, the application of asymptotics on the spectra such as the classical steepest descent path (SDP) method provides diffractive field components as the GTD and the UTD contribution to the far field.

Focusing the attention on (76) with explicit expression obtainable from (70) and (71), we observe that the spectra contain physical singularities related to nonstandard source GO contributions $[I_{ct}(\eta), I_{c\pi t}(\eta)]$ and related to the kernel through ${Y_{t1}}^{-1}(\eta), {Y_{t2}}^{-1}(\eta), Y_c(\eta)$. We also note that (70) and (71) contain nonphysical poles η_n and χ_n (40) and (44) due to the contributions of $H_{ij}(\eta, n)$, $i, j = 1, 2$ and $n \in \mathbb{N}$. These poles are related to nonphysical waveguide modes of parallel PEC waveguides that Green's function procedure shows in the equations although completely canceled/compensated in the final spectral solution.

In order to estimate the total field E_z, we consider the spectral solutions (76) in terms of $V^a_+(\eta), V^a_{\pi+}(\eta)$ and deduce an approximation of the bilateral Laplace/Fourier transform $\upsilon(\eta, y)$ (2) of E_z. Its inversion

$$E_z(x, y) = \frac{1}{2\pi}\int_{-\infty}^{\infty} \upsilon(\eta, y)e^{-j\eta x}d\eta \tag{77}$$

provides in cylindrical coordinate the field

$$E_z(\rho,\varphi) = E^g_z(\rho,\varphi) + E^d_z(\rho,\varphi) + E^s_z(\rho,\varphi) + E^{lk}_z(\rho,\varphi) + E^l_z(\rho,\varphi). \tag{78}$$

In (78), we have GO components $E^g_z(\rho,\varphi)$ (nonstructural poles), possible surface, and leaky waves $E^s_z(\rho,\varphi)$, $E^{lk}_z(\rho,\varphi)$ (structural poles), whereas the branch points are related to lateral waves $E^l_z(\rho,\varphi)$ (structural singularities), and the integral along the SDP is the diffracted component $E^d_z(\rho,\varphi)$.

We also observe that the richest spectral unknowns in terms of physical phenomena are $V_{\pi+}(\eta)$ and $I_{\pi+}(\eta)$ for their definition at the dielectric interface; therefore, in the following, we make reference to these unknowns to examine the impact of structural singularities on the field components.

A. Evaluation of the GO/GTD/UTD Field in Region A

In order to examine GO/GTD/UTD field in region A at far distance, we consider the bilateral spectrum $\upsilon(\eta, y)$ at y = 0 (7) and make reference to the origin of Cartesian axis (Fig. 1). By applying the inverse transform and the SDP method, we capture GO and diffractive components. We note that GO contributions can be obtained either by applying the residue theorem on GO poles to the inverse formula or by the classical GO ray theory

$$E^g_z(\rho,\varphi) = E^i_z(\rho,\varphi) + E^{r1}_z(\rho,\varphi) + E^{r2}_z(\rho,\varphi) \tag{79}$$

where the incident field is $E^i_z(\rho,\varphi)$ (8) and the reflected field from the interface between regions 1, 2, and A is

$$\begin{aligned} E^{r1}_z(\rho,\varphi) &= \Gamma_{d1}E_o e^{jk\rho\cos(\varphi+\varphi_o)}u(\pi-\varphi_o-\varphi) \\ E^{r2}_z(\rho,\varphi) &= \Gamma_{d2}E_o e^{jk\rho\cos(\varphi+\varphi_o)}u(\varphi-\pi+\varphi_o) \end{aligned} \tag{80}$$

with reflection coefficients defined in (95) and (97) and unit step function $u(t)$.

The diffracted contribution derives from the inverse formula applied to the bilateral spectrum (7) [21] while warping the contour integration into the SDP path

$$E^d_z(x, y) = -\frac{1}{2\pi}\int_{SDP} \upsilon(\eta, 0)e^{-j\xi(\eta)y}e^{-j\eta x}d\eta. \tag{81}$$

At far field, we approximate the integral only with the saddle point ($\eta_s = k\cos\varphi$) contribution that provides the GTD

component

$$E_z^{gtd}(\rho,\varphi)=\sqrt{\frac{k}{2\pi\rho}}e^{-j(k\rho-\pi/4)}\upsilon(k\cos\varphi,0)\sin|\varphi| \quad (82)$$

with GTD diffraction coefficient

$$D^{gtd}(\varphi)=\frac{k\upsilon(k\cos\varphi,0)\sin|\varphi|}{jE_o}. \quad (83)$$

The uniformization of (82) gives the diffracted field $E_z^d(\rho,\varphi)$ approximated in the UTD format reported in the following equation:

$$E_z^{utd}(\rho,\varphi)=\sqrt{\frac{1}{2\pi k\rho}}e^{-j(k\rho-\pi/4)}\left[k\,\upsilon(k\cos\varphi)\sin|\varphi| - \frac{1-F\left(2k\rho\cos^2\frac{\varphi_o+|\varphi|}{2}\right)}{2\cos\frac{\varphi_o+|\varphi|}{2}}R\right] \quad (84)$$

where

$$R=jE_o(\Gamma_{d1}-\Gamma_{d2}) \quad (85)$$

is the jump of the reflected rays originated from regions 1 and 2, and $F(z)$ is the Kouyoumjian–Pathak transition function defined in [57] and its application in the framework of WH formulations is reported in [55, eq. (63)].

B. Structural Waves for $x<0$: Surface Waves, Leaky Waves, and Lateral Waves

In the following, we make reference to the analysis of structural field as reported in [58] with a contextualization to the current problem. The structural waves are due to geometrical and material parameters of the problem that implicates singularities in the spectra of the physical quantities. These singularities are present in the kernel of WH formulation and in its reduction to FIEs formulation. In particular, we observe that these singularities are present in the kernel $\underline{\underline{\tilde{M}}}(\eta,\upsilon(hi))$ of (76) and they may contribute to generate surface waves, leaky waves, and lateral waves [32], [33], [34]. In particular, we focus the attention on the spectrum of $V_{\pi+}(\eta)$ for its physical support located at the interface of dielectric and free space. In the explicit equations (70) and (71), we note that the structural singularities of $V_{\pi+}(\eta)$ arise from the analytical properties of the admittances ${Y_{t2}}^{-1}(\eta), Y_{d2}(\eta), Y_c(\eta)$. In particular, they derive from the spectral properties of ${Y_{t2}}^{-1}(\eta)$ (72)

$${Y_{t2}}^{-1}(\eta)=\frac{kZ_o\sin(\xi_d d)}{\xi\sin(\xi_d d)-j\xi_d\cos(\xi_d d)}=\frac{kZ_o\sin(\xi_d d)}{f(\eta)} \quad (86)$$

where $\xi_d=\xi_d(\eta)=\sqrt{k_d^2-\eta^2}$ is the spectral propagation constant in the dielectric medium (28). We relate surface waves and leaky waves to poles of ${Y_{t2}}^{-1}(\eta)$ that are, respectively, proper and improper zeros of $f(\eta)$ [as defined in (86)] when the conventional branch line of $\xi(\eta)$ is selected, i.e., $Im[\xi(\eta)]=0$. However, in the following, we estimate the contributions of structural poles by assuming a branch line of $\xi(\eta)$ the vertical lines from the branch points $\pm k$: ($Re[\eta]=Re[k]$, $Im[\eta]<Im[k]$) and ($Re[\eta]=Re[-k]$, $Im[\eta]>Im[-k]$).

In this problem, we exclude the presence of lateral waves related to the dielectric material. In fact, even if ξ_d is a multivalued function of η with branch points $\pm k_d$, their occurrences in the WH equations and FIEs appear only under $Y_{d2}(\eta)$ that is an even function of ξ_d. This symmetry property cancels the multivalue properties from $Y_{d2}(\eta)$ and, thus, from our formulation and the spectral physical quantities.

To better comprehend the spectral content of $V_{\pi+}(\eta)$, Fig. 3 shows the distribution of singularities in the η-plane for a particular test case with: $k=k_r-jk_r/20$ (with a normalized value $k_r=1$ for illustrative purpose), $\varepsilon_r=5$, and $=0.8\lambda$. The figure illustrates the SDP paths for different observation angles φ, and the vertical branch lines of $\xi(\eta)$ from $\pm k$ and the curves $Re[\xi(\eta)]=0$ and $Im[\xi(\eta)]=0$. The three surface wave poles η_{sn} of the problem are reported with diamond symbols located close to the real axis of η-plane with positive real part bigger than $Re[k]$ and small negative imaginary part, while the first three leaky wave poles η_{lkn} are with positive real part and negative imaginary part reported with five-pointed star symbols located between $Im[\xi(\eta)]=0$ and the vertical branch line of $\xi(\eta)$ ($Re[\eta]=Re[k]$, $Im[\eta]<Im[k]$). Improper poles are not reported since they are related to nonpropagating waves. Moreover, we have omitted to report GO poles $\eta_{go}=-k\cos(\varphi_{go})$ as discussed in (10).

Since we are interested on the inversion of $\upsilon(\eta,0)$ that is defined in terms of $V_{\pi+}(-\eta)$ (7), we need to overturn the complex plane η of Fig. 3 (i.e., the location of poles and other singularities is changed in sign, and thus, they are located in the 2nd quadrant of the complex plane η instead of the 4th one).

The interest on the estimation of structural fields for $x<0$ is twofold: 1) estimation of guided field inside and near the grounded dielectric slab waveguide in Cartesian coordinates and 2) estimation of far field in polar coordinates. For 1), we apply the inverse Laplace transform in the η-plane and the residue theorem, while for 2), we use an asymptotic SDP method as reported in Section VII-A.

Given a pole η_υ of $V_{\pi+}(-\eta)$ or $\upsilon(\eta,0)$, the inversion formula/residue theorem yields the wave $e^{-j\eta_\upsilon x}e^{-j\xi(\eta_\upsilon)y}$ in the free space and $e^{-j\eta_\upsilon x}e^{-j\xi_d(\eta_\upsilon)y}$ in the dielectric medium.

We recall that due to multivalued properties of $\xi(\eta)$ and $\xi_l(\eta)$, we assume as proper sheet the one with $\xi(0)=+k$ and $\xi_l(0)=+k_d$ and as branch lines the vertical lines originated from $\pm k$ and $\pm k_d$.

The surface wave poles of $V_{\pi+}(-\eta)$ in the complex plane η (see overturned Fig. 3) are located in the second quadrant at $-\eta_{sn}$ with $Re[\eta_{sn}]>Re[k]$ and they yield $\xi(-\eta_{sn})$ with negative real part and significant negative imaginary part and $\xi_l(-\eta_{sn})$ with positive real part and small negative imaginary part. As a consequence, the wave associated with surface wave poles exhibits their classical propagation behavior with small attenuation along $x<0$ and strong (small) attenuation along $y>0$ ($-d<y<0$). Considering the equivalent TL modeling of the problem for $x<0$, as done in [58], the behavior of the surface wave structural field for $x<0$ after the Laplace inversion is

$$E_z^{sw}(x,y)=-j\sum_{n=1}^{N_{sw}}Res\left[V_{\pi+}(-\eta),\eta_n^{sw}\right]e^{-j(-\eta_n^{sw})x}\cdot\begin{cases}e^{-j\xi(-\eta_n^{sw})y}, & y>0\\ \dfrac{\sin\left[\xi_d\left(-\eta_n^{sw}\right)(d+y)\right]}{\sin\left[\xi_d\left(-\eta_n^{sw}\right)d\right]}, & -d<y<0\end{cases} \quad (87)$$

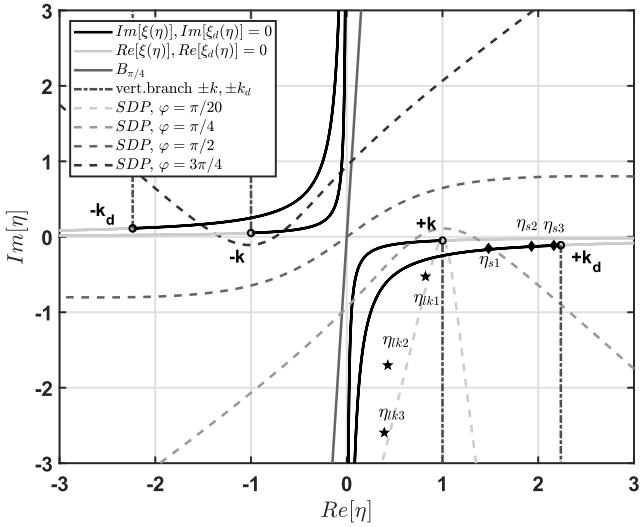

Fig. 3. Spectral plane η with SDP for various observation angles $\varphi = \pi/20, \pi, 4, \pi/2, 3\pi/4$, branch points $\pm k$ ($\pm k_d$) for $\xi(\eta)$ ($\xi_d(\eta)$) multivalued function with vertical branch lines and with curves for $Re[\xi(\eta)] = 0$, $Im[\xi(\eta)] = 0$ ($Re[\xi_d(\eta)] = 0$, and $Im[\xi_d(\eta)] = 0$). In the figure, we have selected $k = k_r - jk_r/20$ and with a normalized value $k_r = 1$ for graphics. $B_{\pi/4}$ is the integration path of the FIEs defined in (74) for $\theta = \pi/4$. For illustrative purpose of the spectral–physical properties of $V_{\pi+}(\eta)$, the figure also reports the location of the structural singularities of $V_{\pi+}(\eta)$ for $\varepsilon_r = 5$ and $d = 0.8\lambda$. We have three surface wave poles η_{sn} with diamond symbols and have reported the three first leaky wave poles η_{lkn} with five-pointed star symbols.

where N_{sw} is the number of surface wave poles η_n^{sw} in $V_{\pi+}(\eta)$ of the problem as, for example, reported in Fig. 3.

The leaky wave poles of $V_{\pi+}(-\eta)$ (see overturned Fig. 3) are $-\eta_{lkn}$, which yields $\xi(-\eta_{lkn})$ and $\xi_l(-\eta_{lkn})$ with positive real part and positive imaginary part. As a consequence, the wave associated with leaky wave poles exhibits their classical propagation behavior with strong attenuation along $x < 0$ and exponentially increases along the y-direction either outside and inside the dielectric medium. In order to highlight the effect on far field of leaky poles, we apply asymptotics using the SDP method. We complete the examination reported in [58] with the theory of [36] and [37] contextualizing the notation and procedure. We first recall that we are dealing with a minus WH unknown $V_{\pi+}(-\eta)$ and a physical support $x < 0$; for this reason, we define the azimuthal angle $\varphi' = \pi - \varphi$. Focusing the attention on one of the $n \in N_{lk}$ leaky poles $\eta_n^{lk} = \beta_n^{lk} - j\alpha_n^{lk}$ ($0 < \beta_n^{lk} < Re[k]$,$\alpha_n^{lk} > 0$), we consider the spectral leaky contribution

$$E_n^{lk} = Res\left[V_{\pi+}(-\eta), \eta_n^{lk}\right]/j \tag{88}$$

that, according to Section II, is related to the field and spectrum

$$E_{z,n}^{lk}(x, y = 0) = E_n^{lk} e^{-j(-\eta_n^{lk})x}, \quad x < 0 \tag{89}$$

$$v_n^{lk}(x, y = 0) = \frac{jE_n^{lk}}{\eta - \left(-\eta_n^{lk}\right)}. \tag{90}$$

Considering equivalent TL for $x < 0$ and applying the inverse Fourier transform (77), we get

$$E_{z,n}^{lk}(x, y) = \frac{1}{2\pi}\int_{-\infty}^{\infty} \frac{jE_n^{lk}}{\eta - \left(-\eta_n^{lk}\right)} e^{-j\xi(\eta)x} e^{-j\eta x} d\eta. \tag{91}$$

The asymptotic estimation of (91), using the SDP procedure applied for GTD contribution, yields in cylindrical coordinates

$$E_{z,n}^{lk}(\rho, \varphi') = \sqrt{\frac{k}{2\pi\rho}} e^{-j(k\rho - \pi/4)} \frac{jE_n^{lk} \sin|\varphi'|}{\cos(\varphi') - \cos\left(\varphi_n^{lk}\right)} \tag{92}$$

with $\eta_n^{lk} = \cos(\varphi_n^{lk}) = \beta_n^{lk} - j\alpha_n^{lk}$. The peak of the leaky wave contribution in the pattern is obtained by maximizing the absolute value of (92), which, in the case of small losses (α_n^{lk}), is approximated with $\cos(\varphi_m') = \beta_n^{lk}/k$.

VIII. Numerical Results and Validation

To validate the proposed technique, we first examine a simplified version of the problem while considering the dielectric material PEC. For this WH problem, the literature presents different and independent solution methodologies. Second, we present a practical test case with dielectric material where all the physical properties of the problem are examined. For this second problem, we make self-convergence tests and validation through an independent fully numerical solution based on the finite-element method (FEM) embedding singular modeling with the following setup: region truncated at a distance of $k\rho = 10$ from the origin O (Fig. 1) with a cylindrical shaped perfectly matched layer (PML) of depth $\lambda/2$ and discretized with second-order triangular elements with a maximum side length of $\lambda/10$.

A. PEC Step Problem for Validation

The PEC step is a simplified version of the problem presented in this article in Fig. 1. The dielectric material is replaced by PEC. In this case, the WH literature offers several independent solutions in the framework of the transversely modified WH equations: Jones' method (see [21, Sec. 6.1.3]) and the reduction to a system of two standard WH equations (see [21, Sec. I.5.1]). This present article provides a third independent WH solution based on the characteristic Green's function procedure, the Fredholm factorization technique, and the completeness of the equations via Cauchy's representations.

The equations obtained in Section VI (69) and (70) are here simplified by the imposition of PEC boundary condition at $x < 0$, $y = 0$ and $x = 0$, $-d < y < 0$, in particular $V_{\pi+}(\eta) = 0$. We obtain that the step problem is modeled by only one nontrivial FIE, i.e., (69). From (69), we remove the integral and the algebraic terms in $V_{\pi+}(\eta)$ and $H_{11}(\eta, n)$ is simplified since $\chi_n \to \infty$, see the definition in the following (44), since the conductivity (as the imaginary part of the permittivity) becomes infinite. We compare the approximated solution of the simplified equation (69) obtained as reported in Sections VI and VII with the one obtainable via Jones's method (see [21, Sec. 6.1.3]) that, starting from the WH equation (see [21, Sec. 10.1]), yields the solution [59]

$$\begin{aligned} V_+(\eta) &= -\sum_{n=1}^{\infty} \frac{jn^2\pi^2 V_+(-\eta_n)}{d^3 k Z_o \eta_n G_+(\eta) G_-(\eta_n)(\eta_n - \eta)} + \frac{G_+(\eta_o)}{G_+(\eta)} V_+^{ns}(\eta) + \\ &\quad - \frac{H(-\eta_o) V_+^{ns}(-\eta)}{G_+(\eta) G_-(-\eta_o)} + \frac{I_+^{ns}(-\eta)}{G_+(\eta) G_-(-\eta_o)} + \frac{I_-^{ns}(\eta)}{G_+(\eta) G_-(\eta_o)} \end{aligned} \tag{93}$$

where $H(\eta) = -Y_{d1}(\eta)$ (27) and $G(\eta) = Y_{t1}(\eta)$ (72), with $V_+(-\eta_n)$ provided by a set of infinite linear system of equations. In Fig. 4, we compare the spectrum of $V_+(\eta)$

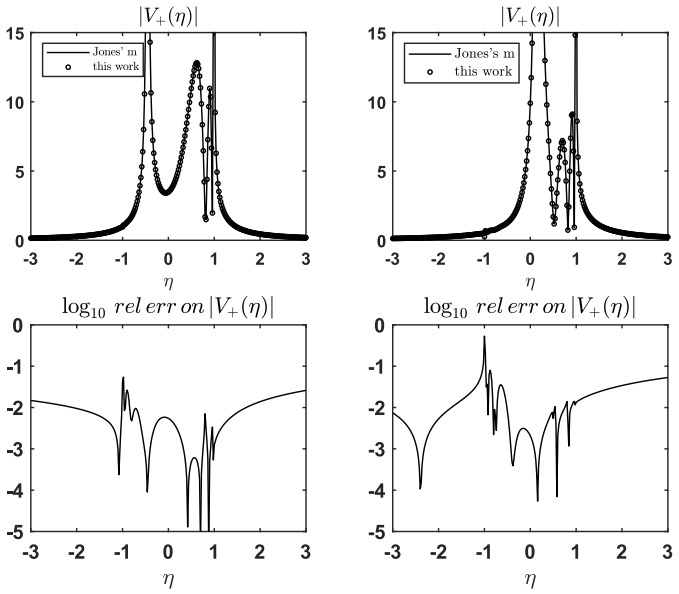

Fig. 4. PEC step problem of Section VIII-A. On top, plots of absolute value of the spectrum $V_+(\eta)$ obtained with Jones' method and this work and on bottom corresponding relative errors between the two solution methods in the $\log_{10}$ scale. The numerical results are obtained for the problems with parameters $k_r d = 11$, $k = k_r - jk_r/10\,000$, and E_z plane wave source with incident angles $\varphi_o = 0.35\pi$ (left), 0.55π (right) rad, and $E_o = 1$ V/m, and with a normalized value $k_r = 1$ for graphics. Numerical results are obtained with discretization parameters $A = 50, h = 0.1, \theta = \pi/4$, and $N = 50$.

obtained with the two methods in two test cases with the following physical parameters: $k_r d = 11$, $k = k_r - jk_r/10\,000$, and E_z plane wave source with incident angles $\varphi_o = 0.35\pi$ and 0.55π rad, and $E_o = 1$ V/m, and with a normalized value $k_r = 1$ for graphics. For the FIE solution of this present article, we select the following discretization parameters in making the linear system (75): $A = 50, h = 0.1$, $\theta = \pi/4$, and $N = 50$ terms of $H_{11}(\eta, n)$ that are selected by considering self-convergence and our experience in handling diffraction problems, see, for instance, [56] and references therein.

For what concerns the solution of (93), we demonstrate that the full convergence of the method is obtained by considering the first $N = 50$ terms of the series. We observe that for an acceptable convergence, we might consider only N terms where N represents a slightly increased number of modes with respect to the number of propagating pseudo-modes η_n (40) of the equivalent parallel PEC plate waveguide. With the physical parameters selected in these test cases, we have three propagating modes and $N = 5$ is sufficient to get acceptable convergence. $N = 50$ terms are useful to obtain cross-convergence between the two methods. Note that N represents both the number of terms of the series (93) and the series on modified (69), and thus, we compare solutions with the same number of correction terms. Fig. 4 shows the plots of absolute value of the spectrum $V_+(\eta)$ obtained with Jones' method and this work, and the relative errors between the two solution methods in the $\log_{10}$ scale that are below/approximately 10^{-2} with an expected increased loss of convergence near $-k$. The spectral solutions are then examined in terms of asymptotic estimates of far field as reported in VII. We observe that in the PEC step problem, only GO (79) and UTD diffraction (84) components are present. We note that spectral errors are smoothed when we perform asymptotic calculus. Thus, since we obtain a relative error below/approximately 10^{-2} in terms of spectrum $V_+(\eta)$ (Fig. 4), in Fig. 5, both the GTD diffraction coefficient (83) and the total far field are with faster cross-convergence with respect to the spectrum, respectively, below 10^{-2} and 10^{-3} (60 dB). We recall that the cross-convergence is obtained by comparing the solutions using Jones' method and this work that completely overlap in Fig. 5 for what concerns the absolute value of the GTD diffraction coefficient and the total far field.

This example (the PEC step) demonstrates the effectiveness of the WH method proposed in this article with cross-convergence with a completely different solution method (Jones' method).

In Section VIII-B, we provide the solution of the semi-infinite grounded slab illuminated by an E_z-polarized plane wave where the alternative WH methods used in the PEC step solution are not applicable.

B. Semi-Infinite Grounded Slab

In this section, we present a test case for validation of this work with physical insights. In particular, we analyze the convergence, the self-convergence, and the validation of the proposed method for the analysis of the structure presented in Fig. 1 with an E_z plane wave illumination. The solution and its convergence are studied in terms of spectral quantities, diffraction coefficients, total far fields, and field components.

In this test case, we consider the following physical parameters: $E_o = 1$ V/m, $k = k_r - jk_r/10\,000$, $\varphi_o = 0.55\pi$ rad, $\varepsilon_r = 4$, and $d = 0.55\lambda$; we assume a normalized value $k_r = 1$ for graphics. The full convergence of the solution of the problem is obtained by applying the discretization method reported in Section VI to (69) and (70). In the following, we consider as a reference solution the one obtained with integration parameters $A = 40, h = 0.1, \theta = \pi/4$, and $N = 5$, where N is the number of the terms considered in the series of (69) and (70) as discussed in Section VIII-A for a quality solution. In Fig. 6, we show the spectrum $v(\eta, y = 0)$ for real η obtained for the reference solution and the relative errors in the log 10 scale obtained with different discretization parameters A and h. The figure demonstrates self-convergence in terms of spectrum. Moreover, we can analyze the physical properties of the solution in terms of peaks of the spectrum. As expected, we have peaks corresponding to the following.

1) GO incident and reflected wave $\eta = \eta_o = -k\cos(\varphi_o) \simeq 0.156 - 0.0000156\,j$.
2) Branch point $\eta = k = k_r - jk_r/10\,000$ ($k_r = 1$).
3) Surface wave $\eta = -\eta_1^{sw} = -1.310 + 0.000261\,j$.
4) Surface wave $\eta = -\eta_2^{sw} = -1.844 + 0.000212\,j$.

We observe that $\eta = \pm k_d$ are not present as discussed in Section VII-B, and the procedure compensates for nonphysical poles as demonstrated by the small spikes near $\eta_{1,2}^{sw}$. The leaky wave poles are not appearing in Fig. 6 since they are far from the real axis in this problem, for example, the first two poles are: $\eta = -\eta_1^{lk} = -0.4605 + 1.063\,j$ and $\eta = -\eta_2^{lk} = -0.4521 + 2.442\,j$. Moreover, the parameters of the problem are not optimized for the excitation of the leaky phenomenon that is beyond the scope of this article. This analysis is coherent with the spectrum reported in Fig. 3 for a different problem (different physical parameters of the problem).

Fig. 7 reports the solution in terms of GTD diffraction coefficient (83) together with analysis of self-convergence for various discretization parameters A and h with respect to the reference solution $A = 40$ and $h = 0.1$. On the left, Fig. 8 reports the solution in terms of field components at

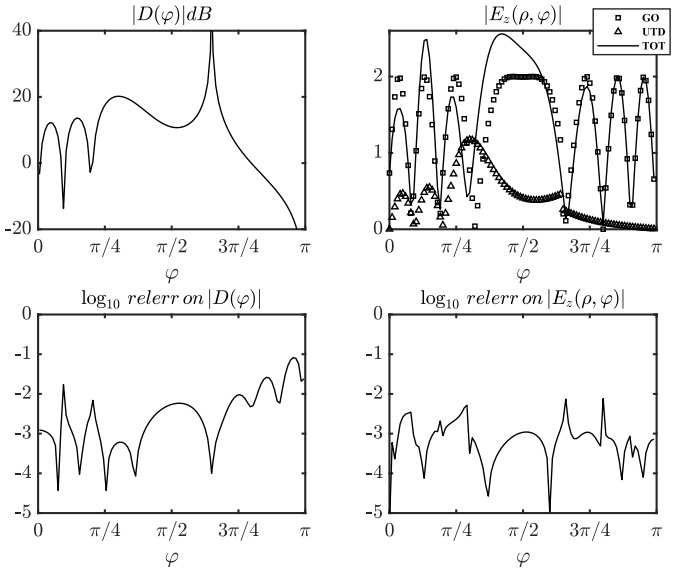

Fig. 5. PEC step problem of Section VIII-A examined using Jones' method and this work. On the top left, GTD diffraction coefficient, while on the top right, the total far field at $k_r\rho = 12$ for $k_r d = 11$, $k = k_r - jk_r/10\,000$, E_z plane wave source with incident angles $\varphi_o = 0.35\pi$ rad, $E_o = 1$ V/m, and with a normalized value $k_r = 1$ for graphics. Numerical results are obtained with discretization parameters $A = 50, h = 0.1$, $\theta = \pi/4$, and $N = 50$ and the two methods completely overlap for what concerns the absolute value of the GTD diffraction coefficient and the total far field. On the bottom left, we have the relative error in the $\log_{10}$ scale of the GTD diffraction coefficient, while on the bottom right, one of the total far fields.

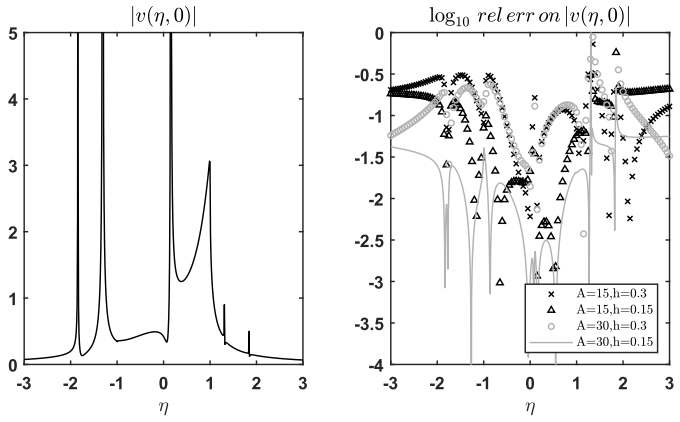

Fig. 6. Semi-infinite grounded slab test case of Section VIII-B with $d = 0.55\lambda$, $k = k_r - jk_r/10\,000$, $\varepsilon_r = 4$, E_z plane wave source with incident angles $\varphi_o = 0.55\pi$ rad, $E_o = 1$ V/m, and with a normalized value $k_r = 1$ for graphics. The reference numerical results are obtained with discretization parameters $A = 40, h = 0.1$, $\theta = \pi/4$, and $N = 5$. On the left, plots of absolute value of the spectrum $v(\eta, y = 0)$ obtained for the reference results, and on the right, corresponding relative errors in the $\log_{10}$ scale between the reference solution and solutions obtained for different discretization parameters A, h. The figure demonstrates self-convergence in terms of spectrum.

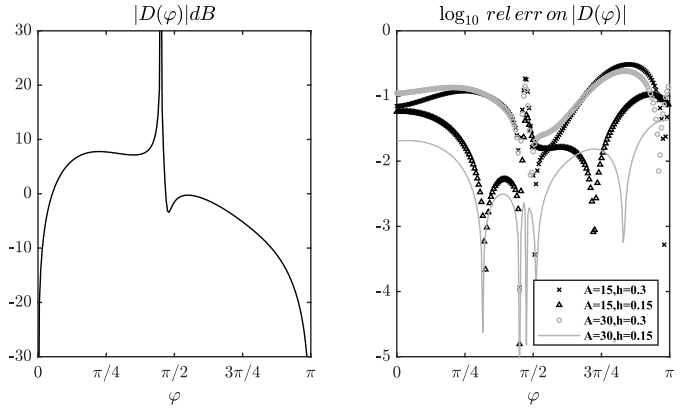

Fig. 7. Semi-infinite grounded slab test case of Section VIII-B. The reference numerical results are obtained with discretization parameters $A = 40$, $h = 0.1$, $\theta = \pi/4$, and $N = 5$, while self-convergence is studied for different discretization parameters A and h. The figure reports: on the left the GTD diffraction coefficient and on the right the relative error in the $\log_{10}$ scale of the GTD diffraction coefficient obtained with different discretization parameters A and h with respect to the reference solution $A = 40$ and $h = 0.1$.

$k_r\rho = 12$ from the origin of Fig. 1: GO component (79), UTD component (84), total far field, and the thereinto total leaky contributions of the first two poles (92). In particular, we note a peak of the GTD diffraction coefficient in Fig. 7 and the finite discontinuity of GO and UTD in Fig. 8 for $\varphi = \pi - \varphi_o = 0.45\pi$ due to the shadow boundary of reflected waves (80). The discontinuity of the GO component is compensated by one of the UTD components yielding continuous total far field at $\varphi = \pi - \varphi_o$. Finally, on the right of Fig. 8, we report an independent validation by comparing the total field of our reference solution with the one obtained by the FEM code [44] with the following setup: region truncated at a distance of $\rho = 10\lambda$ from the origin O with PML of cylindrical shape of depth $\lambda/2$ and quadratic triangular elements with max side length of $\lambda/10$. The agreement between the two solutions is evident, except slightly for particular directions, probably due to the truncation of the geometry and the different truncation condition between free space and the dielectric layer in FEM.

Let us focus the attention on the excited structured field. From Section VII-B, we obtain that the structural field is a summation of structured modes: surface waves and leaky waves according to Fig. 3 although it reports poles for a different problem. In Table I, we reports x-propagation constants η_v [poles of $V_{\pi+}(\eta)$] with the type of structural singularities, the y-propagation constants in free space $\xi(-\eta_v)$, the y-propagation constants in the dielectric medium $\xi_d(-\eta_v)$, and the excitation coefficients, i.e., the residue $Res[V_{\pi+}(-\eta), \eta_v]$ for the two surface waves compatible with the structure and for the first two leaky waves. From Table I, we note that the following conditions hold.

1) The surface wave poles $-\eta_v$ of $v(\eta, y)$ have $Re[\eta_v] > k_r$ (slow wave), $\xi(-\eta_v)$ with negative real part and significant negative imaginary part and $\xi_d(-\eta_v)$ with positive real part and small negative imaginary part. As a consequence, the wave associated with surface wave poles exhibits their classical propagation behavior with small attenuation along $x < 0$ and strong (small) attenuation along $y > 0$ ($-d < y < 0$).
2) The leaky wave poles $-\eta_v$ of $v(\eta, y)$ have $Re[\eta_v] < k_r$ (fast wave), $\xi(-\eta_v)$ and $\xi_l(-\eta_v)$ with positive real part and positive imaginary part typically related to leaky phenomenon.

We note also that the intensity of the first pole for each kind of waves is predominant. The contribution of two first leaky waves is reported in Fig. 8 according to the theory reported in Section VII-B, while Fig. 9 shows the plot of $E_z(x = 0, y)$ related to the two surface waves modes (87) of Table I. We note that, due to the small and similar attenuation of the two surface wave modes along x, the field components remain with the same intensity, and however. due to the phase variation, we have different shapes.

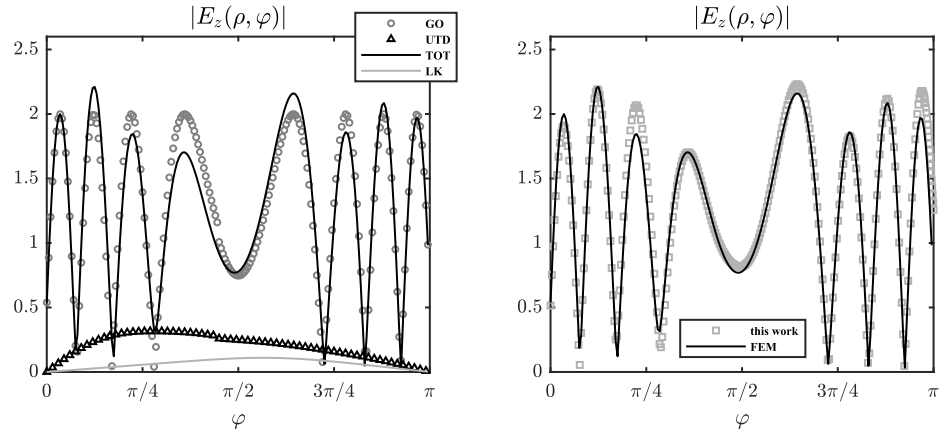

Fig. 8. Semi-infinite grounded slab test case of Section VIII-B. The reference numerical results are obtained with discretization parameters $A = 40$, $h = 0.1$, $\theta = \pi/4$, and $N = 5$, while self-convergence is studied for different discretization parameters A and h. The figure reports: on the left the total far field at $k_r\rho = 12$ for $d = 0.55\lambda$, $k = k_r - jk_r/10\,000$, E_z plane wave source with incident angles $\varphi_o = 0.55\pi$ rad, $E_o = 1$ V/m, and with a normalized value $k_r = 1$ for graphics. The left subfigure reports also the components of field: GO component, UTD component, total far field, and the thereinto total leaky contributions of the first two poles. On the right, we have the validation obtained comparing the total field of our reference solution with the one obtained by the FEM code as described in the main text.

TABLE I

PROPERTIES OF STRUCTURAL WAVES FOR THE TEST CASE ACCORDING TO (87) AND (91)

η_v	type	$\xi(-\eta_v)$	$\xi_l(-\eta_v)$	$Res[V_{\pi+}(-\eta),\eta_v]$
η_1^{sw}=1.30992 - 0.00026 j	surface	-0.00029 - 0.84611 j	1.51132 - 0.00004 j	0.0502378 - 0.222354 j
η_2^{sw}=1.84379 - 0.00021 j	surface	-0.00018 - 1.54906 j	0.77487 - 0.00001 j	-0.033951 + 0.039732 j
η_1^{lk}=0.46053 - 1.06308 j	leaky	1.42680 + 0.34306 j	2.22850 + 0.21951 j	-0.352567 + 0.290859 j
η_2^{lk}=0.45215 - 2.44178 j	leaky	2.63318 + 0.41925 j	3.14343 + 0.35110 j	-0.162793 + 0.0798026 j

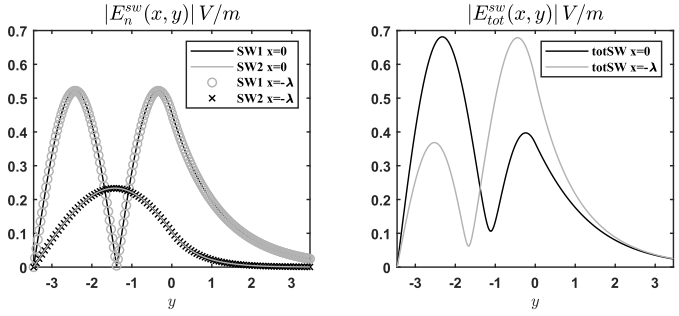

Fig. 9. Surface wave components (left) of the structural field $E_z^{sw}(x, y)$ at $x = 0, -\lambda$ for test case and total surface wave contribution (right).

IX. CONCLUSION

We propose a new methodology to solve the problem of scattering from a truncated grounded slab illuminated by an arbitrarily incident E_z-polarized plane wave. The method is based on an extension of the WH technique that uses the concept of characteristic Green's function and the Fredholm factorization technique. In this article, we demonstrate that the combination of these mathematical tools allows to study the problem in the spectral domain with physical and engineering insights. In particular, the proposed semianalytical solution allows the estimation of field components similar to what is done with closed-form spectral solutions when available. Physical phenomena, such as the reflection, diffraction, and excitation of surface/leaky waves, are reported. Numerical results validate the proposed methodology.

APPENDIX
ESTIMATION OF NS CONTRIBUTIONS

Nonstandard contributions arise in integral representations while applying the Fredholm factorization procedure. These contributions are due to GO contributions in WH unknowns that generate offending poles in the spectra (i.e., located in the regularity half-plane of the WH unknowns, see Section II). By considering plane wave illumination with E_z polarization at normal incidence (9), we need to distinguish two major cases.

Examining GO, for $0 \le \varphi_o \le \pi/2$, we have that $V_+(\eta), I_+(\eta)$ are nonstandard plus functions, while $V_{\pi+}(\eta), I_{\pi+}(\eta)$ are standard plus functions for the location of GO poles and considering the geometrical support for the presence of the field components in the spectra. We also need to consider the properties of $+$ and $\pi+$ unknowns when estimated in $-\eta$ whose poles are located in the reversed half-plane. This property means that, for $0 \le \varphi_o \le \pi/2$, we reflect the regularity properties of WH unknowns estimated in η to the ones in $-\eta$: $V_+(-\eta), I_+(-\eta)$ are nonstandard minus functions, while $V_{\pi+}(-\eta), I_{\pi+}(-\eta)$ are standard minus functions. With reference to Fig. 1, considering the reflection problem at a distance d from the PEC surface with a plane wave illumination (9) at $0 \le \varphi_o \le \pi/2$, we obtain

$$V_+^{ns}(\eta) = j\frac{E_o[1+\Gamma_{d1}]}{\eta-\eta_o}, \quad V_{\pi+}^{ns}(\eta) = 0$$
$$I_+^{ns}(\eta) = = -j\frac{E_o[1-\Gamma_{d1}]}{\eta-\eta_o}\frac{\sin\varphi_o}{Z_o}, \quad I_{\pi+}^{ns}(\eta) = 0 \qquad (94)$$

where the reflection coefficient Γ_{d1} at $y = 0$ is defined by

$$\Gamma_{d1}(\eta) = \frac{Y_c(\eta) - Y_{d1}(\eta)}{Y_c(\eta) + Y_{d1}(\eta)} \qquad (95)$$

evaluated at $\eta_o = -k\cos(\varphi_o)$. The admittances reported in (95) are defined at (14) and (27) and they are derived using TL equivalence for the layered structure problem located at $x > 0$ (regions 1 and A).

While considering $\pi/2 \leq \varphi_o \leq \pi$, we have opposite regularity properties for the WH unknowns, yielding

$$V_+^{ns}(\eta) = 0, \quad V_{\pi+}^{ns}(\eta) = V_-^{ns}(-\eta) = j\frac{E_o[1+\Gamma_{d2}]}{\eta+\eta_o}$$
$$I_+^{ns}(\eta) = 0, \quad I_{\pi+}^{ns}(\eta) = -I_-^{ns}(-\eta) = j\frac{E_o[1-\Gamma_{d2}]}{\eta+\eta_o}\frac{\sin\varphi_o}{Z_o} \tag{96}$$

with the reflection coefficient Γ_{d2} at $y = 0$ defined by

$$\Gamma_{d2}(\eta) = \frac{Y_c(\eta) - Y_{d2}(\eta)}{Y_c(\eta) + Y_{d2}(\eta)} \tag{97}$$

at η_o, with admittances (14) and (36) related to the TL equivalence problem of the layered structure located at $x < 0$ (regions 2 and A).

REFERENCES

[1] W. R. Jones, "A new approach to the diffraction of a surface wave by a semi-infinite grounded dielectric slab," *IEEE Trans. Antennas Propag.*, vol. AP-12, no. 6, pp. 767–777, Nov. 1964.

[2] I. Anderson, "Plane wave diffraction by a thin dielectric half-plane," *IEEE Trans. Antennas Propag.*, vol. AP-27, no. 5, pp. 584–589, Sep. 1979.

[3] R. G. Rojas and P. H. Pathak, "Diffraction of EM waves by a dielectric/ferrite half-plane and related configurations," *IEEE Trans. Antennas Propag.*, vol. 37, no. 6, pp. 751–763, Jun. 1989.

[4] A. D. Rawlins, E. Meister, and F.-O. Speck, "Diffraction by an acoustically transmissive or an electromagnetically dielectric half-plane," *Math. Methods Appl. Sci.*, vol. 14, no. 6, pp. 387–402, Aug. 1991.

[5] T. B. A. Senior and J. L. Volakis, *Approximate Boundary Conditions in Electromagnetics* (IEE Series). London, U.K.: IEE, Mar. 1995.

[6] S. A. Bokhari, J. R. Mosig, and F. E. Gardiol, "Radiation pattern computation of microstrip antennas on finite size ground planes," *IEE Proc. H (Microw., Antennas Propag.)*, vol. 139, no. 3, pp. 278–286, 1992.

[7] S. Maci, L. Borselli, and L. Rossi, "Diffraction at the edge of a truncated grounded dielectric slab," *IEEE Trans. Antennas Propag.*, vol. 44, no. 6, pp. 863–873, Jun. 1996.

[8] C. M. Angulo, "Diffraction of surface waves by a semi-infinite dielectric slab," *IRE Trans. Antennas Propag.*, vol. 5, no. 1, pp. 100–109, Jan. 1957.

[9] P. Gelin, M. Petenzi, and J. Citerne, "Rigorous analysis of the scattering of surface waves in an abruptly ended slab dielectric waveguide," *IEEE Trans. Microw. Theory Techn.*, vol. MTT-29, no. 2, pp. 107–114, Feb. 1981.

[10] L. W. Pearson and R. A. Whitaker, "A transverse aperture-integral equation solution for edge diffraction by multiple layers of homogeneous material," *Radio Sci.*, vol. 26, no. 1, pp. 169–174, Jan. 1991.

[11] V. Volski and G. A. E. Vandenbosch, "Radiation patterns of sources placed near the truncation of a semi-infinite dielectric structure: The demonstration case of a magnetic line current," *IEEE Trans. Antennas Propag.*, vol. 48, no. 2, pp. 240–245, Feb. 2000.

[12] E. Jorgensen, S. Maci, and A. Toccafondi, "Fringe integral equation method for a truncated grounded dielectric slab," *IEEE Trans. Antennas Propag.*, vol. 49, no. 8, pp. 1210–1217, Aug. 2001.

[13] V. A. Volski and G. A. E. Vandenbosch, "Efficient integral equation formulation of diffraction at the edge of a truncated dielectric structure based on PO solutions: Application to the case of arbitrarily polarized line sources," *Radio Sci.*, vol. 38, no. 2, p. 14, Apr. 2003.

[14] C. P. Bates and R. Mittra, "Waveguide excitation of dielectric and plasma slabs," *Radio Sci.*, vol. 3, no. 3, pp. 251–266, Mar. 1968.

[15] A. Ittipiboon and M. Hamid, "Application of the Wiener-Hopf technique to dielectric slab waveguide discontinuities," *IEE Proc. H (Microw., Opt. Antennas)*, vol. 128, no. 4, pp. 188–196, 1981.

[16] K. Uchida and K. Aoki, "Scattering of surface waves on transverse discontinuities in symmetrical three-layer dielectric waveguides," *IEEE Trans. Microw. Theory Techn.*, vol. MTT-32, no. 1, pp. 11–19, Jan. 1984.

[17] K. Aoki, A. Ishizu, and K. Uchida, "Scattering of surface waves in semi-infinite slab dielectric waveguide," *Kyushu Univ. Fac. Eng. Memoirs*, vol. 42, no. 3, pp. 197–215, Sep. 1982.

[18] I. H. Tayyar and B. Çolak, "Plane wave scattering by a dielectric loaded slit in a thick impedance screen," *J. Electromagn. Waves Appl.*, vol. 31, no. 6, pp. 604–626, Apr. 2017.

[19] B. Polat and L. W. Pearson, "Electromagnetic wave scattering from a semi-infinite grounded simple slab," in *Proc. Int. Conf. Electr., Commun., Comput. Eng. (ICECCE)*, Istanbul, Turkey, Jun. 2020, pp. 1–6.

[20] V. Daniele and G. Lombardi, "Fredholm factorization of Wiener-Hopf scalar and matrix kernels," *Radio Sci.*, vol. 42, no. 6, pp. 1–19, Dec. 2007.

[21] V. Daniele and R. Zich, *The Wiener-Hopf Method in Electromagnetics*. Raleigh, NC, USA: SciTech, 2014.

[22] D. S. Jones, "Diffraction by a waveguide of finite length," *Math. Proc. Cambridge Philos. Soc.*, vol. 48, no. 11, pp. 118–134, 1952.

[23] D. S. Jones, "Diffraction by a thick semi-infinite plate," *Proc. Roy. Soc. London A, Math. Phys. Sci.*, vol. 217, pp. 153–175, 1953.

[24] D. S. Jones and M. J. Lighthill, "The scattering of a scalar wave by a semi-infinite rod of circular cross section," *Philos. Trans. Roy. Soc. London A, Math. Phys. Sci.*, vol. 247, no. 934, pp. 499–528, 1955.

[25] B. Noble, *Methods Based on the Wiener-Hopf Technique for the Solution of Partial Differential Equations*. London, U.K.: Pergamon Press, 1958, ch. 5.

[26] M. Hashimoto, M. Idemen, and O. A. Tretyakov, "Some diffraction problems involving modified Wiener-Hopf geometries," in *Analytical and Numerical Methods in Electromagnetic Wave Theory*, K. Kobayashi, Ed. Tokyo, Japan: Science House, 1993, ch. 4, pp. 147–228.

[27] A. Yazici and A. H. Serbest, "Scattering of plane waves by an anisotropic dielectric half-plane," *IEEE Trans. Antennas Propag.*, vol. 47, no. 9, pp. 1476–1484, Sep. 1999.

[28] T. Nagasaka and K. Kobayashi, "Wiener-Hopf analysis of the diffraction by a thin material strip," in *Advances in Mathematical Methods for Electromagnetics*, K. Kobayashi and P. D. Smith, Eds. Stevenage, U.K.: SciTech, 2020, ch. 11, pp. 255–277.

[29] V. Daniele, G. Lombardi, and R. S. Zich, "Diffraction by a truncated slab filled by dielectric material," in *Proc. IEEE Int. Symp. Antennas Propag. USNC-URSI Radio Sci. Meeting*, Atlanta, GA, USA, Jul. 2019, pp. 483–484.

[30] V. G. Daniele, G. Lombardi, and R. S. Zich, "Wiener-Hopf analysis of the scattering from an abruptly ended dielectric slab waveguide," in *Proc. 14th Eur. Conf. Antennas Propag. (EuCAP)*, Copenhagen, Denmark, Mar. 2020, pp. 1–3.

[31] V. Daniele, G. Lombardi, and R. S. Zich, "Radiation and scattering of an arbitrarily flanged dielectric-loaded waveguide," *IEEE Trans. Antennas Propag.*, vol. 67, no. 12, pp. 7569–7584, Dec. 2019.

[32] N. S. Kapany and J. J. Burke, *Optical Waveguide*. New York, NY, USA: Academic, 1972.

[33] D. Marcuse, *Theory of Dielectric Optical Waveguides*. New York, NY, USA: Academic, 1974.

[34] L. M. Brekhovskikh, *Waves in Layered Media*. New York, NY, USA: Academic, 1980.

[35] T. Tamir and A. Oliner, "The influence of complex waves on the radiation field of a slot-excited plasma layer," *IRE Trans. Antennas Propag.*, vol. 10, no. 1, pp. 55–65, Jan. 1962.

[36] A. Hessel, "On the influence of complex poles on the radiation pattern of leaky-wave antennas," *IRE Trans. Antennas Propag.*, vol. 10, no. 5, pp. 646–647, Sep. 1962.

[37] A. A. Oliner and D. R. Jackson, "Leaky-wave antennas," in *Antenna Engineering Handbook*, J. L. Volakis, Ed. New York, NY, USA: McGraw-Hill, 2007, ch. 11.

[38] D. R. Jackson, C. Caloz, and T. Itoh, "Leaky-wave antennas," *Proc. IEEE*, vol. 100, no. 7, pp. 2194–2206, Jul. 2012.

[39] F. Monticone and A. Alù, "Leaky-wave theory, techniques, and applications: From microwaves to visible frequencies," *Proc. IEEE*, vol. 103, no. 5, pp. 793–821, May 2015.

[40] N. Engheta and R. W. Ziolkowski, *Electromagnetic Metamaterials: Physics and Engineering Explorations*. Hoboken, NJ, USA: Wiley, 2006.

[41] P. Baccarelli et al., "Fundamental modal properties of surface waves on metamaterial grounded slabs," *IEEE Trans. Microw. Theory Techn.*, vol. 53, no. 4, pp. 1431–1442, Apr. 2005.

[42] C. L. Holloway, E. F. Kuester, J. A. Gordon, J. O'Hara, J. Booth, and D. R. Smith, "An overview of the theory and applications of metasurfaces: The two-dimensional equivalents of metamaterials," *IEEE Antennas Propag. Mag.*, vol. 54, no. 2, pp. 10–35, Apr. 2012.

[43] B. Friedman, *Principles and Techniques of Applied Mathematics*. New York, NY, USA: Wiley, 1956, ch. 3.

[44] R. D. Graglia and G. Lombardi, "Singular higher order complete vector bases for finite methods," *IEEE Trans. Antennas Propag.*, vol. 52, no. 7, pp. 1672–1685, Jul. 2004.

[45] J. Meixner, "The behavior of electromagnetic fields at edges," *IEEE Trans. Antennas Propag.*, vol. AP-20, no. 4, pp. 442–446, Jul. 1972.

[46] J. Van Bladel, *Singular Electromagnetic Fields and Sources*. Oxford, U.K.: Clarendon, 1991.

[47] W. C. Chew, *Waves and Fields in Inhomogeneous Media*. Piscataway, NJ, USA: IEEE Press, 1990, sec. 1.5.
[48] V. Daniele, G. Lombardi, and R. S. Zich, "The double PEC wedge problem: Diffraction and total far field," *IEEE Trans. Antennas Propag.*, vol. 66, no. 12, pp. 6482–6499, Dec. 2018.
[49] I. D. Abrahams and G. R. Wickham, "On the scattering of sound by two semi-infinite parallel staggered plates—I. Explicit matrix Wiener-Hopf factorization," *Proc. Roy. Soc. London A, Math. Phys. Sci.*, vol. 420, pp. 131–156, 1988.
[50] L. B. Felsen and N. Marcuvitz, *Radiation and Scattering of Waves*. Englewood Cliffs, NJ, USA: Prentice-Hall, 1973.
[51] V. G. Daniele, G. Lombardi, and R. S. Zich, "The scattering of electromagnetic waves by two opposite staggered perfectly electrically conducting half-planes," *Wave Motion*, vol. 83, pp. 241–263, Dec. 2018, doi: 10.1016/j.wavemoti.2018.09.017.
[52] V. G. Daniele, G. Lombardi, and R. S. Zich, "Network representations of angular regions for electromagnetic scattering," *PLoS ONE*, vol. 12, no. 8, 2017, Art. no. e0182763, doi: 10.1371/journal.pone.0182763.
[53] B. Budaev, *Diffraction by Wedges*. London, U.K.: Longman Scient., 1995.
[54] L. V. Kantorovich and V. I. Krylov, *Approximate Methods of Higher Analysis*. Groningen, The Netherlands: Noordhoff, 1964.
[55] V. G. Daniele and G. Lombardi, "Wiener-Hopf solution for impenetrable wedges at skew incidence," *IEEE Trans. Antennas Propag.*, vol. 54, no. 9, pp. 2472–2485, Sep. 2006.
[56] V. Daniele and G. Lombardi, *Scattering and Diffraction by Wedges 2: The Wiener-Hopf Solution—Advanced Applications*. Hoboken, NJ, USA: Wiley, 2020.
[57] R. G. Kouyoumjian and P. H. Pathak, "A uniform geometrical theory of diffraction for an edge in a perfectly conducting surface," *Proc. IEEE*, vol. 62, no. 11, pp. 1448–1461, Nov. 1974.
[58] V. G. Daniele, G. Lombardi, and R. S. Zich, "The electromagnetic field for a PEC wedge over a grounded dielectric slab: 2. Diffraction, modal field, surface waves, and leaky waves," *Radio Sci.*, vol. 52, no. 12, pp. 1492–1509, 2017.
[59] V. Daniele, R. Tascone, and R. Zich, "Scattering from structures involving steps," in *Proc. URSI Int. Electromagn. Symp.*, Santiago de Compostela, Spain, Aug. 1983, pp. 107–110.

Vito Daniele was born in Catanzaro, Italy, in March 1942. He received the Laurea degree in electronic engineering from the Politecnico di Torino, Turin, Italy, in 1966.

In 1980, he was a Full Professor in electrical engineering at the University of Catania, Catania, Italy. From 1981 to 2012, he was a Professor of electrical engineering at the Politecnico di Torino, where he has been an Emeritus Professor since 2015. He has served as a Consultant to various industries in Italy. He has authored or coauthored more than 150 papers in refereed journals and conference proceedings and several textbook chapters. In particular, his studies on the Wiener–Hopf technique have produced the books: *The Wiener–Hopf Method in Electromagnetics* and *Scattering and Diffraction by Wedges: The Wiener-Hopf Solution* (two volumes). His current research interests include analytical and approximate techniques for the evaluation of electromagnetic fields both at high and low frequencies.

Prof. Daniele has been elected as a Corresponding Member of the National Academy of Sciences of Torino since 2013, where he was a National Member in 2021. He was the chairman and an invited speaker for several international symposia. He was a Guest Editor of the Special Issue on Electromagnetic Coupling to Transmission Lines for Electromagnetics in 1988. He is a reviewer of many international journals.

Guido Lombardi (Senior Member, IEEE) was born in Florence, Italy, in December 1974. He received the Laurea degree *(summa cum laude)* in telecommunications engineering from the University of Florence, Florence, in 1999, and the Ph.D. degree in electronic engineering from the Polytechnic of Turin, Turin, Italy, in January 2004.

From 2000 to 2001, he was an Officer of the Italian Air Force, Florence. In 2004, he was an Associate Researcher with the Department of Electronics, Polytechnic of Turin. In 2005, he joined the Department of Electronics, Polytechnic of Turin, as an Assistant Professor with tenure, where he is currently a Full Professor. He was a Visiting Researcher with the Department of Electrical and Computer Engineering, University of Houston, Houston, TX, USA. He was a Programme Organizer at the Newton Institute for Mathematical Sciences (INI), University of Cambridge, Cambridge, U.K., in August 2019. He has authored or coauthored about 100 peer-reviewed scientific publications, including two research monographs published by Wiley/ISTE. His research interests comprise analytical and numerical methods for electromagnetics, Wiener–Hopf method, diffraction, numerical integration, electromagnetic singularities, microwave passive components, and metamaterials.

Dr. Lombardi was an IEEE AP-S AdCom Member for the triennium from 2016 to 2018 and from 2019 to 2021. He is also a Senior Member of the URSI (URSI Senior Individual Membership Recognition). He was a recipient of the Raj Mittra Travel Grant Award for a Junior Researcher at the 2003 IEEE APS International Symposium and USNC/CNC/URSI National Radio Science Meeting, Columbus, OH, USA. In 2018, he was a recipient of the London Mathematical Society Research in Pairs grant as a Research Visitor to the University of Cambridge. He served as a member for the Organizing Committee in the International Conference on Electromagnetics in Advanced Applications (ICEAA) since 2001 and the IEEE-APS Topical Conference on Antennas and Propagation in Wireless Communications (IEEE-APWC) since 2011. He has been the Publication Chair of ICEAA and IEEE-APWC since 2011. He was the AP-S Technical Program Vice-Chair at three editions of the IEEE AP-S International Symposium and USNC/CNC/URSI National Radio Science Meeting in 2019, 2021, and 2022. He served the 2012 and 2015 IEEE AP-S International Symposium and USNC/CNC/URSI National Radio Science Meeting, Chicago, IL, USA, as a Co-Organizer of the Special Sessions on innovative analytical and numerical techniques for complex scattering problems, special materials, and nanostructures. He regularly serves as a reviewer for several international journals on physics, electrical engineering, and electromagnetics, among which IEEE, IET, Wiley, Elsevier, PLoS, OSA, ACES journals, and transactions. He was an Associate Editor of the IEEE TRANSACTIONS ON ANTENNAS AND PROPAGATION from 2016 to 2019, where he has been serving as a Track Editor since 2019. He is an Associate Editor of IEEE ACCESS journal and the *IET Electronics Letters*.

Rodolfo S. Zich (Honorary Member, IEEE) was born in Torino, Italy, in July 1939. He graduated in electronic engineering from the Politecnico di Torino, Turin, Italy, in 1962.

He has been a Full Professor of electromagnetic fields and circuits at the Politecnico di Torino since 1976, where he has been an Emeritus Professor since 2010. He served as a Rector at the Politecnico di Torino from 1987 to 2001. He has extensive international experience: he was a member of the Board of Directors of École Polytechnique de Paris, Palaiseau, France; and the President of Columbus (Association of Latin America and Europe Universities) and the Cooperative Link between Universities for Science, Technology for Education and Research (CLUSTER). He is very active in promoting education and applied research in cooperation with public and private partners. In 1999, he founded the Istituto Superiore Mario Boella, Turin, a research center on information and communication technologies (ICT). He is the author of several papers. His scientific interests are mainly on hybrid analytical numerical techniques in electromagnetic scattering.

Dr. Zich is a member of the National Academy of Science of Turin in 2001. He received the Gold Medal and the First Class Diploma of Merit for Science, Culture and Art, in Italy, in 2007.

Open Access funding provided by 'Politecnico di Torino' within the CRUI CARE Agreement